CONQUERING THE HARSH PLC CHANNEL WITH QC-LDPC CODES TO ENABLE QOS GUARANTEED MULTIMEDIA HOME NETWORKS

By

YOUNGJOON LEE

A DISSERTATION PRESENTED TO THE GRADUATE SCHOOL
OF THE UNIVERSITY OF FLORIDA IN PARTIAL FULFILLMENT
OF THE REQUIREMENTS FOR THE DEGREE OF
DOCTOR OF PHILOSOPHY

UNIVERSITY OF FLORIDA

2013

To my parents and family

ACKNOWLEDGEMENTS

First and foremost I would like to mention the deep appreciation to my advisor, Prof. Haniph Latchman. He enthusiastically and continually encourages my study and research works. It has been an honor to be his Ph.D. student, and I appreciate his plentiful research advice and contributions.

My gratitude is also extended to all committee members, Prof. Antonio Arroyo, Prof. Janise McNair, and Prof. Richard Newman. I am very appreciative of their willingness to serve on my committee and their valuable advice.

I also thank my lab colleagues at Laboratory for Information Systems and Tele-communications (LIST). Our research discussion and your help were precious for my research progress. I will also never forget our memories in Gainesville.

Last, but certainly not least, I must acknowledge with tremendous and deep thanks my family and parents. The scholastic life of my father has promoted my research desire. Furthermore, without his unconditional support, my doctoral degree is never acquired. Most of all, I would like to thank and have great admiration for the love, sacrifice and education of my last mother.

TABLE OF CONTENTS

Page

LIST OF TABLES

Table Page

LIST OF FIGURES

Figure Page

Abstract of Dissertation Presented to the Graduate School
of the University of Florida in Partial Fulfillment of the
Requirements for the Degree of Doctor of Philosophy

CONQUERING THE HARSH PLC CHANNEL TO ENABLE QOS GUARANTEED MULTIMEDIA HOME NETWORKS

By

Youngjoon Lee

May 2013

Chair: Haniph A. Latchman
Major: Electrical and Computer Engineering

Powerline Communication (PLC) is one of the most promising candidates for use in home network technologies. Although the powerline was originally designed for electrical power transmission at 50 or 60 Hz, it is also possible to transmit broadband signals at higher frequencies. One of the most attractive features of PLC is its whole house accessibility because a large number of powerline outlets are available in typical homes and offices.

This dissertation is mostly focused on multimedia communication and home networks on PLC channel. First, we investigate generally available home networking standards and technologies such as HomePNA, MoCA, HomePlug AV, IEEE 802.11, G.hn, and IEEE P1905. Then, their advantages and disadvantages are compared in terms of data rate, QoS, accessibility, costs, and security. In order to guarantee QoS for PLC multimedia networks, a modified CSMA/CA MAC algorithm is proposed. The proposed MAC algorithm is based on the IEEE 802.11e and the HomePlug 1.0 MAC protocol. Despite the advantageous of PLC there are several hurdles to achieving reliable high speed communications over the Garth PLC channel conditions. For example, one of the typical features of the powerline channel is impulsive noise which degrades the PLC performance. Therefore, we first propose an impulsive noise mitigation scheme with a threshold setting algorithm. Then, LDPC codes with adaptive multi-carrier OFDM

are applied to improve the bit error rate of our system on powerline channels. The comparison between LDPC codes and turbo codes is simulated with different block sizes. Finally, QC-LDPC codes are designed for better error correcting efficiency with less memory storage. The main advantages of the encoding procedure for QC-LDPC codes are their ease of implementation and relatively simple structure. QC-LDPC codes using various block sizes and code rates are compared. We also compare turbo codes with QC-LDPC codes with G.hn standard on real PLC channels. When SNR is 2 dB or more, error rates of (8640,4320) QC-LDPC code are 10 percentage or less of error rates of turbo code.

CHAPTER 1
ERROR CONTROL CODES WITH ADAPTIVE OFDM AND MAC ALGORITHM FOR MULTIMEDIA DATA ON PLC

Home network is a local area network connecting with PC, TV, and any other home appliances within a house. Because it is possible to control home appliances and share multimedia contents, the interest of home networks has become pervasive. Several standards and technologies were proposed and designed for home networks previously. Notable standards are Home Phoneline Networking Alliance (HomePNA) with phoneline, Multimedia over Coax Alliance (MoCA) with coaxial cable, HomePlug AV with powerline, IEEE 802.11n and Ultra Wideband (UWB) with wireless, and G.hn with multiple mediums [1].

In order to realize home networks with seamless services, technical review is required. We investigated and compared home networking standards and technologies with several categories such as data rate, QoS, accessibility, deployment cost, and security. This work is an overview of home network technologies and helpful to understand their advantages and disadvantages.

Medium Access Control (MAC) layer is a sublayer of the data link layer on OSI 7 layer model. MAC sublayer controls the channel access of participating terminals and nodes in a network such as WLAN. Therefore all nodes can share the medium within the multiple access networks. HomePlug 1.0 standard adopted a priority supporting algorithm of Carrier Sense Multiple Access with Collision Avoidance (CSMA/CA). The CSMA/CA mechanism is the contention based system with Backoff Count (BC) between the nodes within same networks. Only the nodes with higher priority frames join in the contention with HomePlug 1.0 MAC algorithm. HomePlug AV applied a hybrid CSMA/TDMA MAC for multimedia traffic. There are two types of modes for HomePlug AV standard. For the reliable QoS of demanding AV, connection oriented Contention Free (CF) service based on periodic TDMA is one mode. The

other mode is the prioritized Contention based service with modified existing CSMA/CA and a four-level priority scheme. The legacy IEEE 802.11 applied both Distributed Coordination Function (DCF) mode based on the CSMA/CA and Point Coordination Function (PCF) mode [2], [3]. IEEE 802.11e uses Hybrid Coordinator Channel Access (HCCA) for CFP and both Enhanced DCF Channel Access (EDCA) and HCCA for CP at a same time.

In order to improve multimedia data rate, we propose a modified CSMA/CA MAC protocol for PLC. The proposed MAC protocol model is based on the IEEE 802.11e and HomePlug 1.0, and allocates the priority to multimedia traffic such as video data.

Impulse noise is short burst noise with single impulse or a series of impulses. Due to the impedance of home appliances, it is a common noise on powerline channel. Because impulsive noise influence on whole frequency spectrum, it deteriorates the performance of multi-carrier systems [4], [5]. Therefore, impulsive noise modeling and analysis should be preceded for powerline technology. The notable impulsive noise modeling schemes on PLC channel were introduced in [6], [7], [8]. The impulse detection on time domain is described in [9]. The algorithm on the frequency domain with additional FFT and IFFT is designed in [10].

In order to mitigate impulsive noise, many algorithms and modulation schemes have been researched previously. The impulsive noise clipping scheme with some thresholds have been highly considered [11], [12]. There are two common methods to assign proper thresholds. One method setting a threshold is based on the upper limit and lower limit with the ADC inputs. Another scheme is based on the proportional level of the average received signal power. The performance of proportional level threshold method is better, but it requires more memory and computations.

For impulsive noise detection, we propose a universal impulsive noise detection algorithm with the threshold mathematically computed using the actual characteristics of impulsive noise in PLC systems. It is an iterative threshold setting algorithm using signal envelope. This proposed algorithm can be applied to various cases of impulsive noise on PLC networks.

Discrete Multitone (DMT) system is an application of OFDM using efficient bit-loading scheme with the available bandwidth. The Inverse Fast Fourier Transform (IFFT) for modulation and the FFT for demodulation are required for DMT. Because each subchannel is orthogonal to other subchannels with OFDM, they are nearly independent and the independence degree increases with the number of subchannels [13]. According to the channel condition, each subcarrier of OFDM uses different modulation schemes. The modulation of HomePlug AV specification is based on BPSK, QPSK, 8-QAM, 16-QAM, 256-QAM, and 1024-QAM with maximum 10 bits [26]. In order to design PLC system, we adopted DMT with adaptive bit loading scheme.

LDPC codes are linear block codes which consist of a parity check matrix with sparse 1's in rows and columns. LDPC codes are first designed by Gallager [14] in 1960. It is possible to perform near Shannon limit which is the theoretical maximum for a symmetric memory less channel. However, LDPC codes are ignored and not realized until 1990s because of the lack of computational effort for code implementation. Tanner designed LDPC code with a proposed graphical representation, a Tanner graph [15]. Tanner graph is a bipartite graph, and it is possible to express the code completely and describe decoding algorithm effectively. In the mid 1990s, McKay, Luby, and others [16], [17], and [18] resurrected error correcting codes with sparse matrices such as LDPC codes. Gallager recognized the decoding advantages of such LDPC

codes and he proposed a deciding algorithm for the BI-AWGNC and a few others for the BSC. These algorithms received much scrutiny in the past decade, and are still being studied.

Turbo codes, which were first introduced in 1993 [19], became one of the most widely adopted codes for Forward Error Correction (FEC) and replace trellis codes by Ungerboeck [20]. Because of high performance, turbo codes are applied in various applications such as 3G mobile, satellite and powerline communications. The theoretical performance of turbo codes is closed to the Shannon Limit like LDPC codes. Turbo codes involve block codes with rows and columns in a rectangular array of bits. There are two kinds of codes, Parallel and Serial Concatenated Convolutional Codes (PCCCs and SCCCs). Basically the turbo encoder is configured with two or more convolutional encoders connected with pseudo-random interleavers. The iterative soft decision algorithm is used for turbo decoder which consists of two or more convolutional decoders. HomePlug AV standard also applied turbo codes for FEC [26]. Several LDPC codes are applied for the error control coding of the proposed system on PLC channel. Moreover, we compare LDPC codes with typical turbo codes with simulation results.

In order to improve forward error correction efficiency, we propose and design new Quasi-Cyclic (QC)-LDPC codes with various block sizes and code rate. A QC code which is a linear block code over GF(2) is generated by circulant permutation process. Because the parity check matrix of QC-LDPC codes consists of arrays of circulant permutation matrices from a base matrix, the memory requirement is decreased dramatically. Therefore, the encoding implementation is relatively easy with simple structure. For the decoding procedure of QC-LDPC codes, soft decision with sum-product algorithm and hard decision with bit-flipping algorithm are considered. As we adopt real PLC channels and noise data which are collected

from a test house, more practical simulation results are expected. Moreover, QC-LDPC code simulation is implemented with G.hn standard.

This report is organized as follows. In Chapter 2, Home network standards and technologies are introduced and compared with technical reviews. In Chapter 3, we propose QoS augmented CSMA/CA MAC protocol for high speed multimedia PLC. In Chapter 4, a novel impulsive noise mitigation algorithm is proposed. Chapter 5 presents LDPC codes with adaptive multi-carrier OFDM for PLC channel. LDPC and turbo codes are also compared. QC-LDPC code design for real PLC channel are described in Chapter 6. Finally, the future research works are presented in Chapter 7.

CHAPTER 2
PLC - A COMPETITIVE CANDIDATE FOR MULTIMEDIA COMMUNICATION AND HOME NETWORKING

2.1 Introduction

In the past, a network has been regarded as an interconnection only between computers. Therefore, network solutions have been properly developed for computer environment. However, as time passed, users have desired to access internet and digital multimedia contents at any other places, not one computer room, in their houses. It would be convenient if we could use the internet in the kitchen, share the HDTV in every room, and play video games with multiple users over network. Moreover, households which own more than one computer are pervasive.

As a result, home networks have become a remarkable issue. Home network is a local area network with PC, TV, and any other home appliances within a house. Thus, since all devices are connected to other devices, users could easily control home appliances and enjoy digital contents anywhere.

We need reliable network services and standards to realize home networks, which demand high data rate and seamless QoS. Deployment costs, convenient access, and security are also important facts for dependable home networks. There are various home networking services [1], [21]. Chapter 2 is organized as follows. The section 2.2 introduces feasible standards and related associations. The technical review is developed in section 2.3. Then, we compared characteristics of standards and media in section 2.4. This work is an overview of home network technologies and helpful to understand their advantages and disadvantages.

2.2 Home Networking Standards

2.2.1 HomePNA

Home Phoneline Networking Alliance (HomePNA) is an association which provides a home network over the regular phoneline. HomePNA is initially designed to transmit digital data

between computers but it becomes one of the most prospective home network standards now. HomePNA 3.1 is the most recent version and received approval by the International Telecommunication Union (ITU) standard [22], [23].

2.2.2 MoCA

Multimedia over Coax Alliance (MoCA) utilizes the coaxial cable for a home network. MoCA was first constituted in 2004, and 10 promoters, 10 contributors, and many associations participate in development as members now. MoCA 1.1 is the most recent version implemented and MoCA 2.0 is under development for the next generation of MoCA standard [24].

2.2.3 HomePlug AV

HomePlug Powerline Alliance is an association of home network over installed powerline. It is established in 2000 and the largest association of powerline network. HomePlug Powerline Alliance designed HomePlug AV standard to support distribution of multimedia data such as HDTV and VoIP throughout home. HomePlug AV2 is under development and the alliance plans to complete the specification within 2010. HomePlug AV2 devices will be designed to interoperate with HomePlug AV devices [25] and [26].

2.2.4 IEEE 802.11n

IEEE 802.11n is an emerging wireless networking standard because of its better performance than previous IEEE 802.11b and IEEE 802.11g. From 2007, IEEE 802.11n products have been certified by Wi-Fi Alliance which is a non-profit organization for high speed WLAN standard [27]. As Wi-Fi Alliance improves interoperability issues, IEEE 802.11n products are compatible with previous WLAN equipment.

2.2.5 Ultra Wideband

Ultra wideband (UWB) is another rising wireless technology for home network. It is possible to play or exchange data of a digital camcorder, HDTV, portable MP3 player, and

mobile computer. UWB is adopted as IEEE 802.15.3a standard for Personal Area Network (PAN). However, IEEE 802.15.3a group terminated development in 2006. European Computer Manufacturers Association (ECMA), a standard organization, specifies UWB physical and Medium Access Control (MAC) standard [28]. ECMA operates for information and communication standard. ISO/IEC approved ECMA UWB specifications based on WiMedia UWB radio platform in 2005 [29].

2.2.6 G.hn

G.hn is the next generation home network standard developed by ITU. G.hn multimedia data is possible to be transmitted over any available home wires such as coaxial cable, powerline, and phoneline. Moreover, according to HomeGrid, which is an industry group supporting G.hn, it can be compatible with other home network standards like HomePlug, HD-PLC, MoCA, and HomePNA. G.hn architecture and physical layer specification is approved in 2009 [30]. Data link layer is also specified and supposed to be approved within 2010.

2.3 Home Networking Technology

2.3.1 Phoneline Network

Because phoneline networking uses the existing phoneline infrastructure, any extra wiring is not required and deployment costs can be reduced. Even though HomePNA share the existing phoneline, it does not disrupt other services such as telephone, fax and DSL services because of different bandwidth allocation. Voice PSTN, DSL, and HomePNA occupy 30~3400 Hz, 30K~1.1 MHz, and 5.5~9.5 MHz bandwidth respectively.

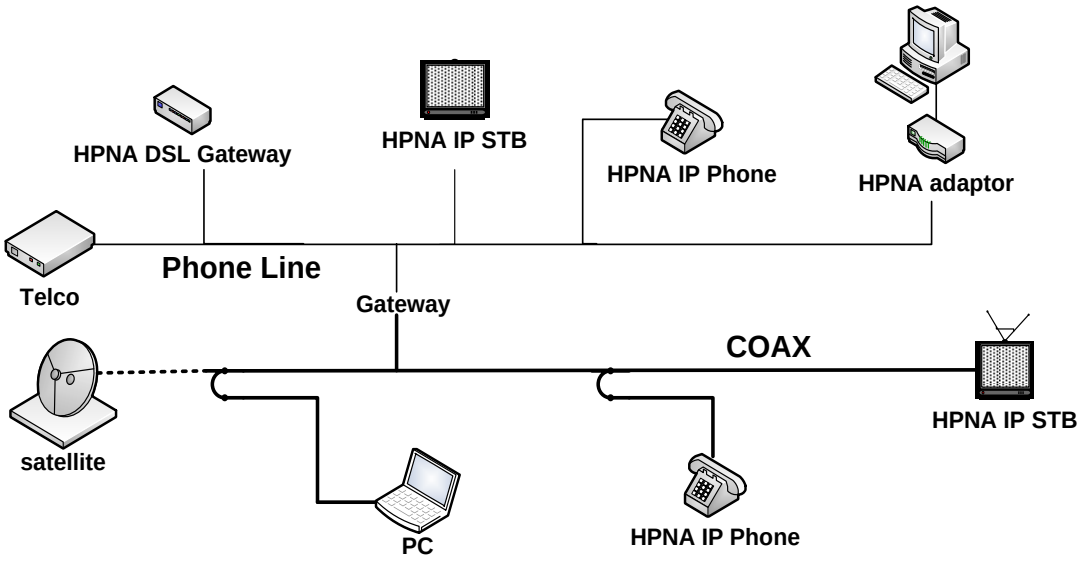

Figure 2-1. An example of HomePNA configuration

There is an example of HomePNA configuration in Figure. 2-1. If the coaxial cable is already installed in the building, it could be also used as a home networking backbone. HomePNA gateway can connect phoneline with coaxial cable. HomePNA 3.1 provides high speed internet service, VOIP and entertainment data including IPTV with MPEG4 over both phoneline and coax at speeds up to 320 Mbps [31]. Moreover, users can easily access wireless signal bridged to the HomePNA backbone, providing internet services and cordless phones. The devices can be up to 1000 feet (300 meters) apart.

QAM modulation is adopted for physical layer of HomePNA. However, physical layers over phoneline and coax support each different spectral modes and bands. Phoneline provides two different modes. Spectral mode A supports 4-20 MHz band range with 2, 4, 8, 16 M band rates, and spectral mode B uses 12 -28 MHz band range with same band rate. On the other hand, the coaxial network adopts 4 different modes. Band ranges are 4-20 MHz, 12-28 MHz, 36-52 MHz, and 4-36 MHz. Band rates are also 2, 4, 8, 16 M band except the last mode which uses one more band, 32 M band [32].

In order to avoid collision between transmissions with robust QoS, HomePNA 3.1 MAC applies a resource reservation scheme. One node in the network operates as a master node and the other nodes become endpoints. The master node arranges the transmission schedule and sends a Media Access Plan (MAP) to endpoints. MAP has transmission opportunity (TXOP) order and nodes with TXOP are permitted to transmit data. If only one node has TXOP, this node occupies the medium. However, if TXOP is allocated to multiple nodes simultaneously, Carrier Sense Multiple Access with Collision Avoidance (CSMA/CA) is invoked to allocate the transmission opportunity with same medium. The carrier sensor in each node detects the start and end of currant transmission to escape collisions. All nodes which want to join a network and transmit data should register with the master node for admission control and security reason. Shared private key encryption scheme is also applied for the network security. Therefore, a node without shared private key is not allowed to transmit data and receive network data [32].

The main disadvantage is the shortage of telephone outlets in houses because it needs a telephone outlet near every unit to access the broadband signal. Therefore, users need to install more wiring and telephone outlets at all locations where they want to access a home network.

2.3.2 Coax Network

Because an estimated 90 percent of TV households in U.S. are already wired for coaxial cable, deployment costs can be saved. Therefore, coax can be used for data connections to TV set top boxes, and other multimedia devices without new connections using MoCA. Moreover, it has appropriate environments to provide IPTV because MoCA technology is inherently based on IP over coax [33].

MoCA adopts 50 MHz flexible bandwidth spectrum between 860~950 MHz frequency band. The bandwidth of MoCA is shown in Figure. 2-2. Because MoCA uses the open spectrum bandwidth, MoCA signal is not interfered with cable and satellite signals which occupy the

bandwidth in the 5~860 MHz and 950~2150 MHz respectively. MoCA 1.1 provides DVD quality entertainment services throughout the home with 270 Mbps rate and high QoS. During the field test, more than 95 percent of cable outlets could deliver broadband signals with 170 Mbps MAC rate and latency was less than 5 milliseconds. MoCA 2.0 intents to improve the data rate up to 1.4 Gbps maximum physical data rate and 800 Mbps of actual throughput [24], [34].

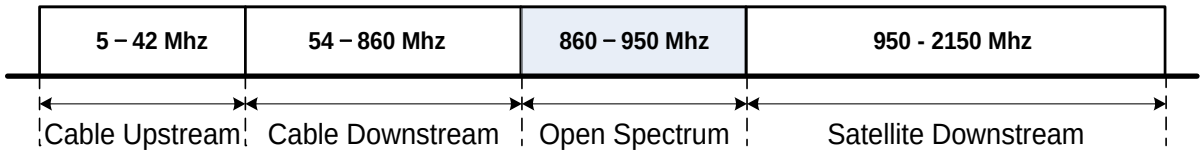

Figure 2-2. MoCA spectrum

In order to optimize the physical rate for any channel, MoCA adopts the pre-equalize modulation with bitloaded Orthogonal Frequency Division Multiplexing (OFDM). Up to 256 QAM constellation is used on each subcarrier for adaptive multitone. Channel profile optimizes preamble and cyclic prefix for multicarrier efficiency. Additionally, Reed Solomon FEC is used for low packet error rate without costs of excessive code redundancy.

All nodes use the same carrier for transmit and receive with Time Division Multiple Access (TDMA). The network control node which is randomly assigned exists to improve MAC efficiency and it controls all transmission with MAP and manages encryption keys. Therefore, the network controller allocates a transmission slot by request-grant mechanism. Selection is based on pre-assigned priorities and the most advantageous locations during network control operation. As the bandwidth is reserved at each flow, MoCA 1.1 supports parameterized QoS (PqoS) [35].

For the security and privacy, transmission signal is encrypted by 56 bit Data Encryption Standard (DES), and traffic keys are rotated. Password is also required for network admission. Main drawback is insufficiency installed cable outlets like phoneline network.

2.3.3 Powerline Network

Powerline Communication (PLC) uses the existing electrical wiring as the network backbone so new line is completely not required. The powerline was originally designed to deliver electrical power at 50~60 Hz. It is also possible to transmit digital signals at high frequency with PLC technology. Since a lot of powerline outlets are available in houses, the access of PLC networks is much easier than other network solutions. A typical house in the U.S. has more than 40 powerline outlets.

HomePlug AV can offer High Definition Television (HDTV) using 2~28 MHz frequency bandwidth. The maximum channel data rate of HomePlug AV is 200 Mbps and the maximum information rate is 150 Mbps. The target physical and MAC data rate of HomePlug AV2 are 1 Gbps and 600 Mbps respectively.

The basic structure of a HomePlug AV OFDM transceiver is described in Figure. 2-3. There are two FEC ways, AV Frame Control FEC and AV Packet Body FEC, at transmitter. AV data from MAC layer gets into AV packet body FEC which consists of scrambler, turbo convolution encoder, and interleaver. After that, the output from FEC passes through mapper, IFFT, insert preamble, and Cyclic Prefix for OFDM modulation. Then the signal is sent to powerline medium by Analog Front End (AFE). At the receiver, AFE, Time Synchronization module, and Automatic Gain Controller (AGC) process the received signal before demodulation. The rest blocks operate with the inverse process of the transmitter for demodulation and FEC [26].

HomePlug AV modulation is based on adaptive bit loading OFDM, which allows efficient bandwidth use and higher maximum data rate. According to the channel condition, each subcarrier of OFDM uses 7 different modulation schemes with BPSK, QPSK, 8-QAM, 16-QAM, 256-QAM, and 1024-QAM. Information bits per carrier also vary from 1 bit to 10 bits, which

depend on modulation schemes. Besides, turbo and Reed-Solomon codes which are concatenated with convolution codes are adopted for forward error correction [25].

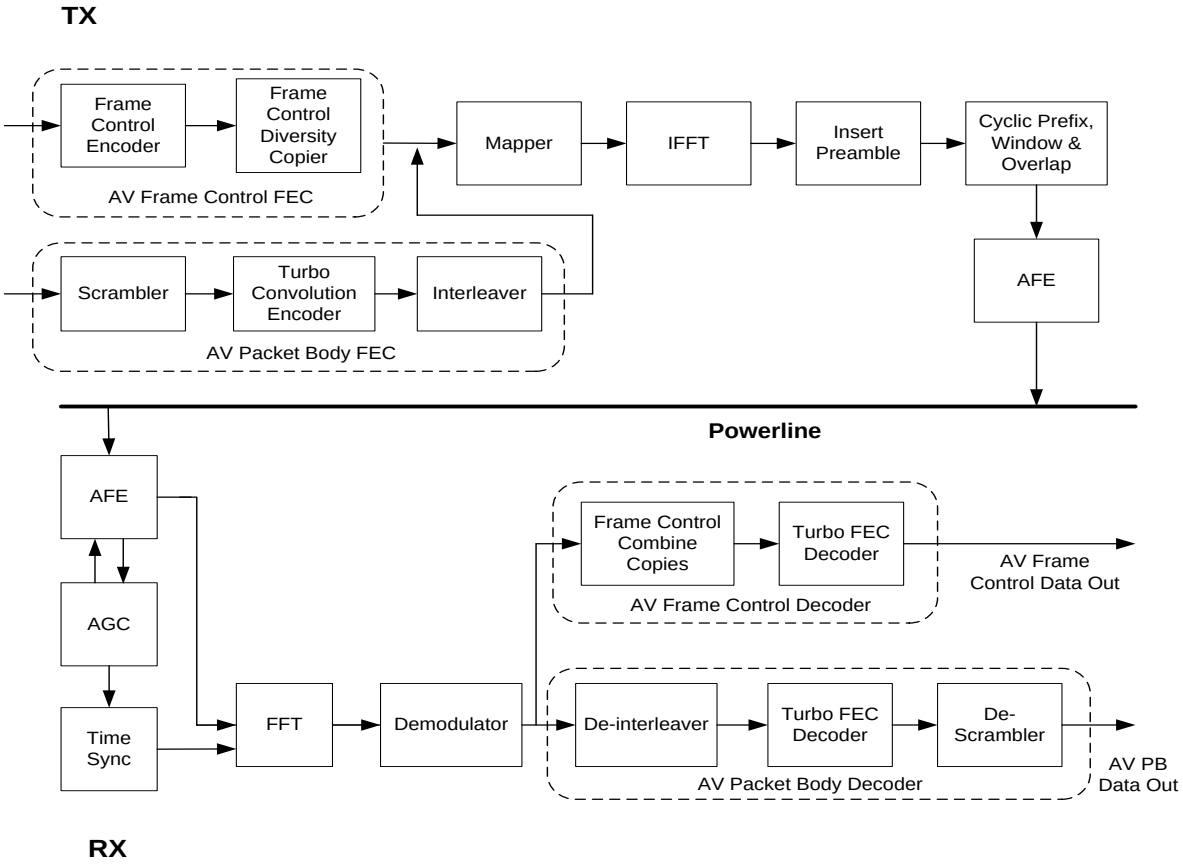

Figure 2-3. The basic structure of a HomePlug AV transceiver

MAC protocol of HomePlug AV adopts two types of communication services with centrally managed architecture. The reliable QoS of demanding video and IP applications is guaranteed through connection oriented Contention Free (CF) service based on periodic TDMA. Central Coordinator (CCo) allocates the channel to nodes and determines the transmission duration. HomePlug AV also uses prioritized Contention based service with modified existing CSMA/CA and a four-level priority scheme. The highest priority traffic nodes contend for transmission opportunity in the contention period [36], [37]. MAC segmentation and MAC Protocol Data Unit (MPDU) is shown in Figure. 2-4. MAC frame is composed of a header,

optional Arrival Time Stamp (ATS), and Check Sum with MAC Protocol Service Unit (MSDU) received from convergence layer. MAC frame consists of 512 octet segments and each segment is encapsulated into a PHY Block (PB) in MPDU. After a receiver receives PBs and restores MSDUs from PBs, it sends Selective Acknowledge (SACK) and requests the retransmission of damaged blocks [26].

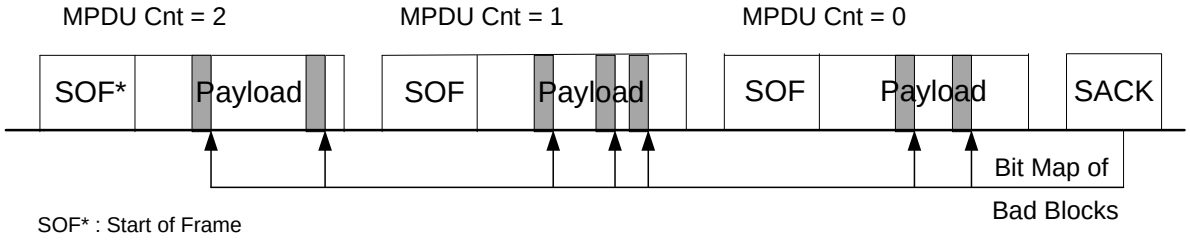

Figure 2-4. HomePlug AV MAC segmentation

For the network security, HomePlug AV adopted 128 bit Advanced Encryption Standard (AES) encryption. It is worked on individual segments and uses the Network Encryption Key (NEK). NEK is used to encrypt data during segmentation in the MAC and may be dynamically changed.

The main drawback of PLC is that interference and noise from home appliances deteriorate network performance. However, channel condition can be improved and PLC is feasible with advanced digital signal processing, forward error correcting codes, and modulation technologies.

2.3.4 Wireless Network

If users consider the mobility, wireless is the most convenient medium because it does not need any wire. However, wireless signals are weakened as the distance between transmitters and receivers grow. There are two outstanding standards for a home network.

2.3.4.1 IEEE 802.11n

The performance IEEE 802.11n is better than previous IEEE 802.11b and IEEE 802.11g. Most of all, the channel width is increased from 20 MHz to 40 MHz to provide higher data rate. The estimated maximum data rate is 600 Mbps, which is almost 9 times faster than IEEE 802.11g. We compared notable IEEE 802.11x characteristics in Table 2-1.

Table 2-1. Characteristic comparison of IEEE 802.11x series

	802.11a	802.11b	802.11g	802.11n
Max. data rate	54 Mbps	11 Mbps	54 Mbps	600 Mbps
Modulation	OFDM	DSSS/CCK	DSSS/ CCK	DSSS/CCK /OFDM
RF band	5 GHz	2.4 GHz	2.4 GHz	2.4/5 GHz
Channel width	20 MHz	20 MHz	20 MHz	20/40 MHz
Range(Indoor)	25 m	35m	25 m	70m
Range(Outdoor)	75m	100m	75m	250m

For the high data rate, IEEE 802.11n adopts Multiple Input Multiple output (MIMO) system, which applies multiple transmitters and receivers to enhance the network performance. Antenna diversity technology can coherently resolve receiving data from multiple signal paths, which ingenerate interference between multipath signals and degrade the ability of receivers. Spatial multiplexing can spatially multiplex numerous independent data, transmitted simultaneously within one spectral channel of bandwidth.

The indoor data range is 230 feet (70 meters) which is variable according to the number and type of walls. However, the outdoor data range is 820 feet (250 meters) with one wall. IEEE 802.11n covers both 2.4 GHz and 5 GHz RF band. Furthermore, IEEE 802.11n adopts three modulation methods such as OFDM, Direct-Sequence Spread Spectrum (DSSS), and Complementary Code Keying (CCK) for compatibility with previous standards [27].

MAC layer is based on previous 802.11 standards, but is advanced with frame aggregation and block acknowledgement. In order to reduce the protocol overhead of frame

headers and inter frame gaps, 802.11n chooses frame aggregation scheme which combines several short frames into one frame. Therefore, the MAC layer efficiency can be improved. The Aggregated MAC Service Data Unit (A-MSDU) extends the size of MAC and physical frames from 2304 bytes to 8 Kbytes and from 2304 bytes to 64 Kbytes respectively. The block acknowledgement scheme is a protocol which sends a block acknowledgement (ACK) frame instead of several ACK frames [38], [39].

IEEE 802.11n security mechanism inherits robust security of IEEE 802.11i which is specially implemented for enhanced security. For high data rate, Wi-Fi Protected Access Version 2 (WPA2) is utilized. IEEE 802.11n data is also encrypted by AES.

2.3.4.2 Ultra wideband

UWB uses wider frequency spectrum and lower power than any other wireless technology so it can transmit large amount of digital data and reduce the interference with other wireless spectral signals. In addition, UWB can enable long battery life of mobile units with low costs. The allocated bandwidth is 500 MHz or 20% of the center frequency band. Furthermore, Federal Communications Commission (FCC) authorizes the unlicensed frequency band between 3.1~10.6 GHz to UWB. The data rate is variable from 100 Mbps to 2 Gbps which depends on the distance between devices. The maximum data rate is much faster than other standards. Nevertheless, the problem of UWB is that data rate is rapidly decreased as the UWB devices have more distance. The transmit power is -41dBm/MHz so the applicable bandwidth is 1.3 GHz wide pulse within 0.75 feet (23 centimeters) but it is reduced to 500 MHz at 2 feet (60 centimeters) apart. Furthermore, the maximum data range is very short, 30 feet (9 meters) [28]. The UWB network is configured as Ad-hoc connections so every UWB devices can be both a sender and receiver. Moreover, it is possible to transmit multiple streams to multiple devices simultaneously.

ECMA separates UWB spectrum to 14 bands and a frequency bandwidth of each band is 528 MHz. These 14 bands are arranged with 5 band groups. 4 band groups consist of 3 bands each, and the other group has 2 bands. Different band group is exploited depending on application types. MultiBand OFDM (MB-ODFM) is adopted with 110 subcarriers per band to transmit signal. Depending on time domain spreading, frequency domain spreading, and FEC code scheme, different data rate is applied such as 53.3 Mbps, 80 Mbps, 106.7 Mbps, 160 Mbps, 200 Mbps, 320 Mbps, 400 Mbps, and 480 Mbps. ECMA uses convolutional code for FEC with code rate of 1/3, 1/2, 5/8, and 3/4 [29].

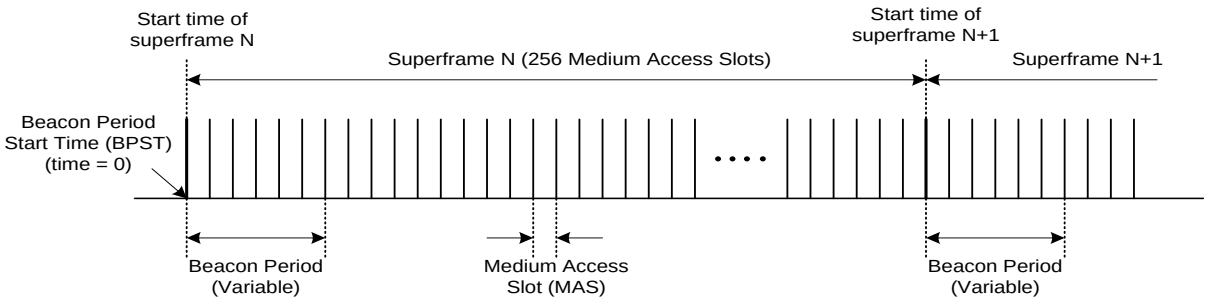

Figure 2-5. UWB MAC superframe structure

The MAC protocol configuration of UWB enhances device mobility so a group of devices can communicates without interruption during grouping and splitting from other devices. UWB selects CSMA and TDMA to utilize prioritized schemes for asynchronous and isochronous data transfer. Moreover, a Distributed Reservation Protocol (DRP) is adopted to occupy the medium with TDMA, and Prioritized Contention Access (PCA) with CSMA is used for network scalability. UWB defines the timing structure called MAC superframe structure in Figure. 2-5. The superframe is divided into 256 Medium Access Slots (MASs) and the duration of each MAS is 256. In order to coordinate devices in a network, beacons support network timing and medium access reservation of devices. There are three ways for medium access - devices sending beacon

frames during the BP, devices participation in the reservation sending frames during reservations, or using a prioritized contention based access [29].

UWB devices authenticate each other for security. AES-128 Cipher Block Chaining Message Authentication Code algorithm (CCM) is provided for privacy. UWB also use replay attack prevention measures with Secure Frame Counters (SFCs) and replay counters [29].

2.3.5 Hybrid - G.hn

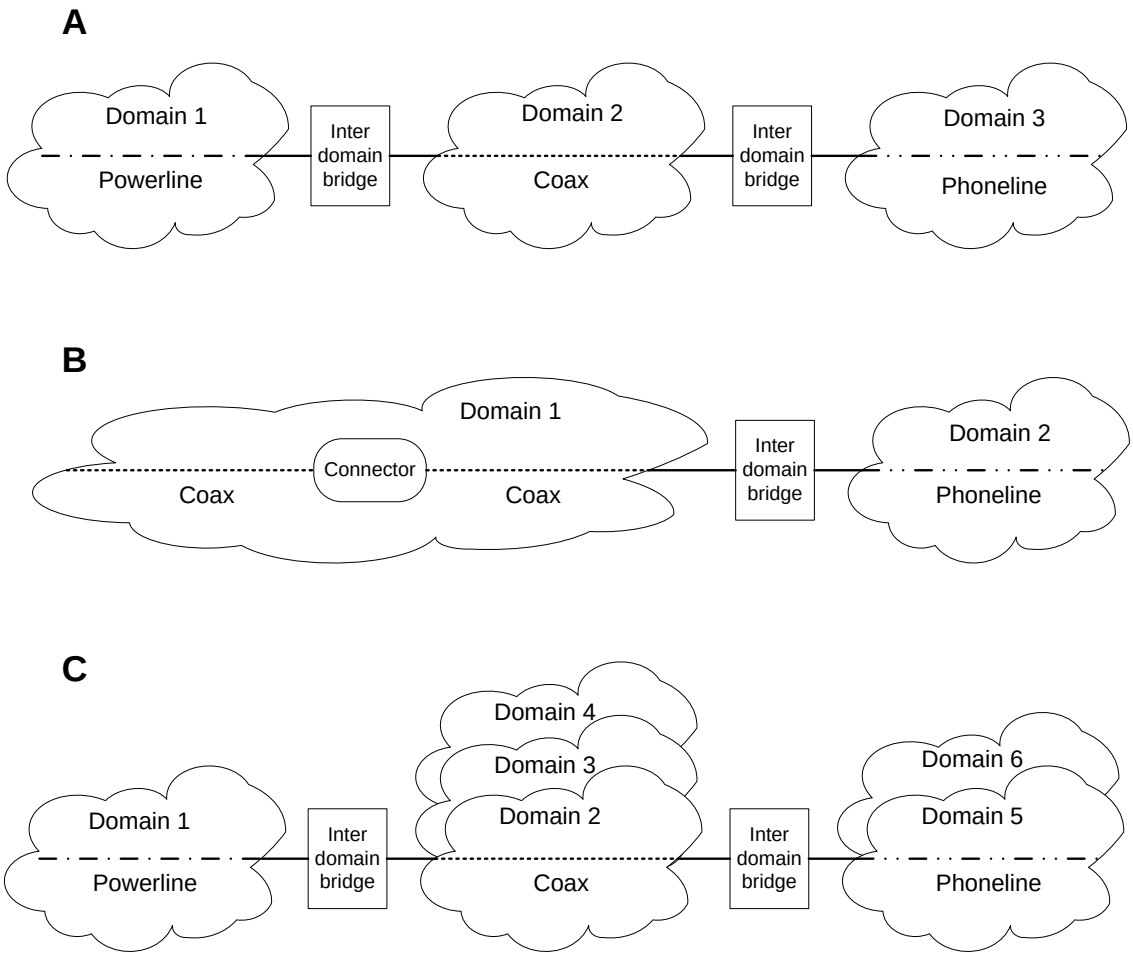

Figure 2-6. G.hn configuration

G.hn utilizes any possible coax, phoneline or powerline as networking medium with 1 Gbps, which is target data rate. Three examples show the configuration between domain and

medium of G.hn in Figure. 2-6. Each domain allocates a single medium. Coax, phoneline and powerline, are possessed of three each domains in Figure. 2-6-A. Inter-domain bridges connect a domain to another domain. Figure. 2-6-B shows another network which comprises coax and phoneline. Two coax segments are linked with a connector in domain 1 which is connected to domain 2 by an inter-domain bridge. It is also possible that one or more domains exist in a medium. As shown in Figure. 2-6-C, domain 2, 3, and 4 are combined in the coax medium, and domain 5 and 6 are in the phoneline medium. These domains on each individual medium must adopt orthogonal signals over different frequency bands to escape interference [30].

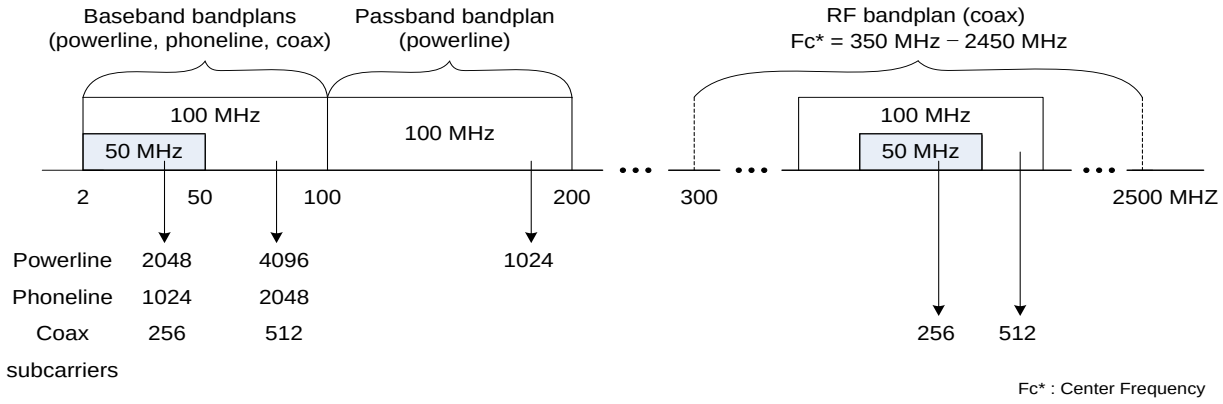

Figure 2-7. G.hn frequency bandplans

Physical layer of G.hn chooses windowed OFDM with the flexible number of subcarriers, which vary with $N = 2^n$, n = 8-12, and $F_{SC} = 2^k \times 24.41$ kHz, k = 0, 1 … 4 respectively. The number of subcarriers with various subcarrier spacing are determined based on channel characteristics. Frequency bandwidth is divided into three bandplans which are Baseband, Passband, and RF bandplans shown in Figure. 2-7. A set of OFDM parameters is used at each medium and bandplan so same subcarrier spacing is allowed in overlapping bandplans. According to the bandplan and medium type, the number of subcarriers is decided. Furthermore, adaptive bit loading algorithm is adopted so data bits of each subcarrier vary from 1 to 12 bits. A

Quasi-Cyclic Low Density Parity Check (QC-LDPC) code is selected for FEC. QC-LDPC codes of G.hn operate with five different code rates such as 1/2, 2/3, 5/6, 16/18, and 20/21 with two block sizes such as 120 and 540 bytes [40].

MAC protocol of G.hn chooses synchronized media access. Domain Master (DM) coordinates all nodes in same domain, and allocates TXOPs to nodes who want to transmit data. Therefore, all nodes can synchronize with the MAC cycle and transmit data during the TXOPs received from DM without collision. Three TXOPs are defined by depending on application types. First, only one node is permitted to transmit data with Contention free TXOP (CFTXOP). It is for fixed bandwidth with QoS guarantee such as video data transmission. Second, Shared TXOP with managed time slots (STXOP) using CDMA/CA is for services with flexible bandwidth for VoIP, interactive video, and games. The other is Contention based TXOP (CBTXOP) in which nodes need to contend for transmission. This type is appropriate for services with different priority levels [40].

G.hn adopts Diffie-Hellman algorithm and the Counter with CCM using 128 bit AES for security. Those are authentication schemes in order to prevent the network from the outside invasion. Encryption key is also used for the security between users in the network [40].

2.4 Comparisons

Until now, we have inquired into several technology options for the multimedia home networks. In order to choose appropriate home networking technology, we need to compare each characteristic with the others. The evaluation criteria are data rate, QoS, accessibility, deployment costs, and security. Home network standards are briefly compared in table 2-2.

First of all, data rate is important because of the huge traffic size of multimedia contents including HDTV signals. The required minimum capacity of basic services is 30 Mbps. The maximum data rates of all home network solutions are greater than 200 Mbps which is enough to

transmit multimedia signals. Data rates of standards are compared in Table 2-2. Specially, UWB and IEEE 802.11n can support a maximum of 2 Gbps and 600 Mbps respectively. However, the data rate of wireless technology is dramatically dropped as the communicating devices become more distant. 1 Gbps data rate of G.hn is the target data rate on the draft.

QoS is also a primary factor for real-time streaming multimedia applications which need seamless bit rate. The network control mechanisms can guarantee the required performance of the data transmission and support different priority to different applications with reliable QoS. Moreover, high QoS technology can diminish delay, jitter, latency, dropped packets, and errors. Phoneline and coax can guarantee users relatively seamless QoS since home network signal is isolated from other voice or data signals using different bandwidth. However, the QoS of PLC is degraded due to the noise and impedance from home appliances within same electrical circuit. Furthermore, the QoS of wireless technology could possibly become vulnerable, because the signal strength and data rate are decreased when the signals pass through walls or the length between devices are extended. Interference with other wireless signals can degrade the QoS too.

Another issue of concerns is the convenience of network access. Even if coaxial cable and phoneline are already installed in most houses, the home networking access is not easily deployed on account of the lack of their outlets. Therefore, users have to reconnect coaxial cable or phoneline all around the houses and perforate the walls to place outlets at every room. On the other hand, powerline outlets are enough for both home networking devices and home appliances. Even one room has several power outlets so it is very handy to access the network. As a matter of fact, wireless is the most convenient method to access the network with completely no wire. Accordingly, wireless technology can remove the complex connecting cables and boost the

mobility of home networking devices. The accessibility of G.hn is also good because users can access any possible nearby wired medium.

The deployment costs should not be disregarded either. The chipset prices between each technology are not much different. Users have to pay money for the installation of extra cables and outlets due to the insufficient connecting outlets of coax or phoneline network. Because powerline and outlets are widely installed in houses, deployment expense is comparatively cheap. However, external PLC adapter is needed at each connection [31]. A deployment cost of wireless technology is high. Wireless users should spend extra costs for access points and transceiver antennas. G.hn uses any wired medium so the cost for installing wires and outlets is cheap. However, users should pay the cost applying gateways between coax, powerline, and phoneline.

Table 2-2. Comparison between home network standards

	Data Rate	QoS	Accessibility	Deployment Costs	Security and privacy	Medium
HomePNA 3.1	320 Mbps	Good	Moderate	Good	Good	Phoneline & Coax
MoCA 1.1	270 Mbps	Good	Moderate	Good	Good	Coax
HomePlug AV	200 Mbps	Moderate	Good	Best	Good	Powerline
IEEE 802.11n	600 Mbps	Moderate	Best	Moderate	Moderate	Wireless
UWB	100 M - 2Gbps	Moderate	Best	Moderate	Moderate	Wireless
G.hn	1 Gbps	Good	Good	Good	Moderate	Phoneline, Coax & Powerline

Finally, security and privacy are very significant because home networking signals contain not only public broadcast signals but also private contents. Each technology has their selected or designed security scheme to enhance the network security and privacy. The security of phoneline, coax, and powerline is somewhat weak because network users share the medium

with neighbors. Therefore, filters between networks are required for isolation. The security of wireless is comparatively weaker than the others. The reason is that wireless signals are spread all around and high frequency spectrum of IEEE 802.11n and UWB is unlicensed. G.hn is possibly exposed to intruders because data signal spreads across coax, powerline, and phoneline.

2.5 Conclusions

There are a number of home networking network solutions and standard associations such as HomePNA with phoneline, MoCA with coax, HomePlug AV with powerline, IEEE 802.11n and UWB with wireless, and G.hn with multiple solutions. In Section 2.3, we investigated home network standards and technologies for multimedia services. We also compared and analyzed data rate, QoS, accessibility, deployment cost, and security of each technology.

It is not easy to state which technology is the best since no technology satisfies all the necessary conditions for a home network, and each of them has their strengths and weaknesses. However, G.hn and HomePlug AV are excellent examples of home network standards to provide multimedia and home network solution. The reason is that they use powerline for the backbone of network medium which requires no new line for their services.

CHAPTER 3
QOS AUGMENTED CSMA/CA MAC PROTOCOL FOR HIGH SPEED MULTIMEDIA PLC

3.1 Introduction

Wireless communication networks have become extremely popular because of their convenience and mobility. Recently, the speed and capacity of WLAN have been substantially improved because of the advanced channel modulation techniques. Furthermore, it has become more feasible to transmit real-time multimedia data such as images, voices, and even videos using the IEEE 802.11e protocol. However, WLANs suffer from overall stability problems common to wireless channels that share spectrum with other interfering applications.

In contrast, Powerline Communications (PLC) has been shown to be substantially more stable while also offering speeds approaching 1 Gbps [1], [21]. Powerline Communication uses the existing electrical wire for the network medium and has the notable advantage of accessibility and convenience. Chapter 3 seeks to combine desirable features of the IEEE 802.11e protocol with the HomePlug 1.0 PLC Carrier Sense Multiple Access (CSMA) protocol in an effort to improve the over performance on the PLC channel. In this regard it should be noted that while the HomePlug AV standard does offer a hybrid CSMA/TDMA MAC to support multimedia traffic, almost all implementations to date provide only CSMA support that uses the HomePlug 1.0 standard. Thus it is of independent research interest to investigate the augmentation of HomePlug 1.0 with IEEE802.11e QoS features.

First, we will describe the main characteristics and functions of the IEEE 802.11 and IEEE 802.11e in Section 3.2. We also review the access mechanism of HomePlug 1.0 for powerline communication [22]. We propose a new multimedia MAC protocol for high speed powerline communication based on the IEEE 802.11e and HomePlug 1.0 in Section 3.3. Then

proposed scheme is compared to typical HomePlug MAC and simulation results are shown in Section 3.4. Conclusions are represented in Section 3.5.

3.2 Related Works

3.2.1 Priority Mechanism of IEEE 802.11

The legacy IEEE 802.11 is supporting both Distributed Coordination Function (DCF) mode based on the CSMA/CA and Point Coordination Function (PCF) mode for reliable QoS [23], [31]. IEEE 802.11 MAC frame structure for access mechanism is shown in Figure. 3-1.

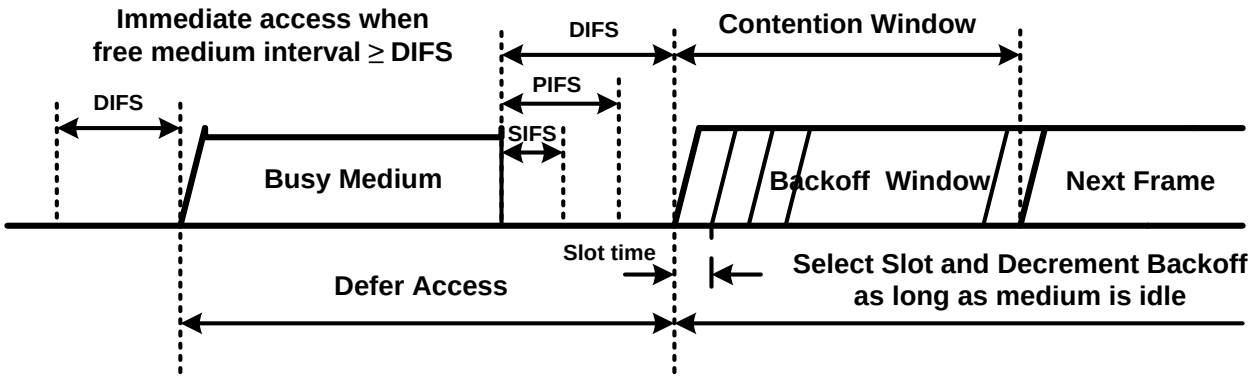

Figure 3-1. Access mechanism of IEEE 802.11

DCF uses a CSMA/CA mechanism for supporting data traffic service. When the medium is idle during DCF Inter Frame Space (DIFS), all data nodes set a random backoff counter with the range of 0~CW. Whenever slot time passes, nodes decrease counter by 1. When the counter becomes 0, the node transmits a frame. When nodes meet a busy channel before the counter becomes 0, they return to the first step with current backoff counter in order to support priority increment.

PCF is a function for supporting time-bounded service like voice traffic which is optional. When the channel is idle during PCF Inter Frame Space (PIFS) which is shorter than DIFS, Access Point (AP) polls directly the transmission node without contention. Under this operational mode the channel consists of a series of super frames. A super frame consists of

Contention Free Period (CFP) with PCF mode and Contention Period (CP) with DCF mode. A super frame has to contain DCF mode which can transmit one MAC Service Data Unit (MSDU) at least.

Problems of IEEE 802.11 for guaranteeing QoS are as follows:

- Not guaranteeing QoS of real-time traffic because all traffic nodes have same opportunity to access channel with the same condition using DCF mode only.
- Not satisfying QoS requirements because PCF mode for QoS supporting uses polling scheduling mechanism based on the round-robin.
- Shorter super frame, higher overhead from polling.

IEEE 802.11e seeks to solve these problems of 802.11.

3.2.2 Priority Supporting Mechanism of HomePlug 1.0

HomePlug 1.0 basically uses a priority supporting mechanism of Carrier Sense Multiple Access with Collision Avoidance (CSMA/CA) which may be seen as an augmentation of the IEEE 802.11 wireless LAN [32], [33]. All nodes of typical CSMA/CA can join in the contention from set a Backoff Count (BC) whenever they meet an idle time of Contention Inter Frame Space (CIFS). However, only the nodes having higher priority frames join in the contention with HomePlug 1.0 MAC algorithm. Figure. 3-2 is the frame structure of HomePlug 1.0 MAC, which has the following key features for priority setting:

- Supports 4 priority class based on the traffic characteristics: CA3, CA2, CA1, and CA0. CA3 & CA2 means High Priority (CA3: Voice, CA2: Video), and CA1 & CA0 means Low Priority (CA1: Best Effort Data, CA0: Background Data).
- Uses Deferral Count (DC) in order to minimize the loss from collision.

After the end of last transmission, nodes having a frame to transmit join in the Priority Resolution Period (PRP) whenever they meet an idle time of Contention Inter Frame Space (CIFS). Whenever nodes having high priority frames set PRS0 at PRP, all nodes having low priority frames revert to a HOLD mode. The priority decision between voice and video is solved

at PRS1 stage. If PRS1 is set, video nodes become HOLD otherwise video nodes have transmission opportunities. If PRS0 is not set, data transmission is available.

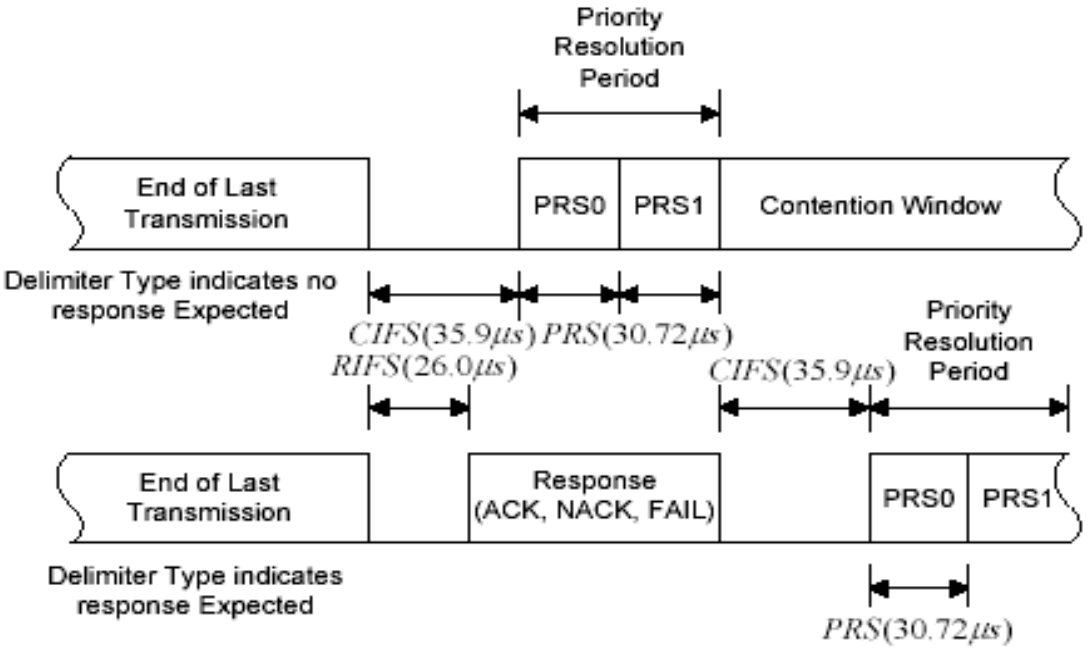

Figure 3-2. Basic operation mechanism of HomePlug 1.0

The basic operation mechanism of HomePlug 1.0 MAC is as follows:

- Only the nodes having frame class specified by PRP (Priority Resolution Period), PRS0 or PRS1, join in the medium access contention.
- Contention nodes set a random BC with the range of [0~CW].
- Nodes joining in the contention decrease own BC by 1 whenever idle time slot passes.
- When BC becomes 0, if medium is still idle then node transmits a frame.
- When medium is busy before BC becomes 0, node returns to the first step and waits for idle time of CIFS which is HOLD state.
- HOLD state node uses old decreased BC as it stands not new one in order to increase own priority. More number of HOLD, higher priority.
- Also HOLD state node sets a DC. DC is defined by both the number of HOLD and the frame's priority which is specified by standard document.
- HOLD state node decreases BC and DC by 1 after PRP.

- If BC=0, transmit a frame. If DC=0, set a new BC with larger range CW in order to minimize collision probability.

The problems of HomePlug 1.0 for guaranteeing the QoS characteristics are as follows:

- There is high frame loss probability of video traffic, having lower priority but requiring higher transmission speed than voice when the network has higher traffic load.
- During the voice node's transmission, video frames arrive with various arrival rates to the waiting queues of video nodes. When the video nodes have opportunities for transmission, only contention based medium access is used without considering any priority mechanism.

3.2.3 QoS Guaranty Mechanism of IEEE 802.11e

IEEE 802.11 defines Access Category (AC) and specifies a back-off mechanism operating independently based on the AC. While IEEE 802.11 uses PCF mode for Contention Free Period and DCF mode for Contention Period, IEEE 802.11e uses Hybrid Coordinator Channel Access (HCCA) for CFP and both Enhanced DCF Channel Access (EDCA) and HCCA for CP at a same time. IEEE 802.11e MAC frame details are shown in Figure. 3-3.

In EDCA Mode, each node have 4 independent queues for 4 ACs, which are AC_VO (Voice), AC_VI (Video), AC_BE (Best Effort) and AC_BK (Background), and operate back-off mechanism independently to access medium. Each AC has different parameter values, such as Arbitration Inter Frame Space (AIFS) and CW in order to support priority mechanism flexibly. The AC having high priority can access channel with high priority by assigning lower value of AIFS, CW_{min}, and CW_{max}. TXOPLimit Parameter means a transmittable frame time at some instant of time. The AC of a transmission node that wins a channel contention has this Transmission Opportunity (TXOP) parameter, and the node can transmit multiple frames during DefaultTXOPLimit within every Short Interframe Space (SIFS) time interval.

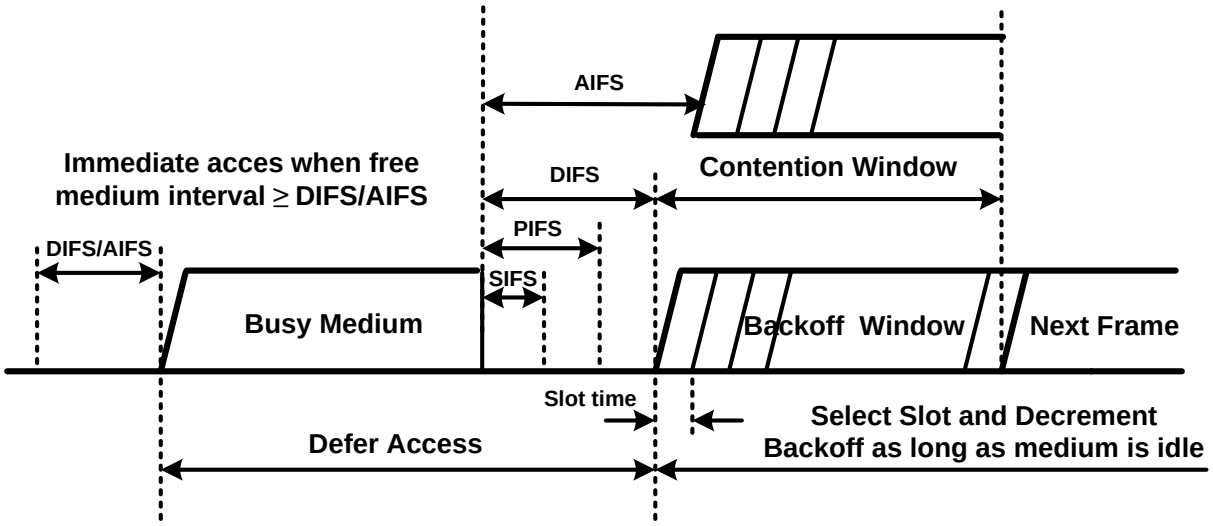

Figure 3-3. Access mechanism of IEEE 802.11e

In HCCA mode, real-time traffic nodes have an opportunity of channel usage based on the polling mechanism of AP like PCF mode in IEEE 802.11. QoS parameters are transferred between AP and real-time traffic node. A real-time node granted by AP can transmit multiple frames based on the TXOPLimit.

3.2.4 Connections with IEEE P1905.1

The IEEE P1905.1 working group for Convergent Digital Home Networks (CDHNs) with heterogeneous technologies supports existing wireless and wire standards such as IEEE 802.11 (Wi-Fi), IEEE 1901 (HomePlug), IEEE 802.3 (Ethernet), and Multimedia over Coax(MoCA). Since Powerline and Wi-Fi are the most widely available media in typical homes, the results of Chapter 3 will provide a seamless mechanism to provide equivalent QoS in this converged environment. If Ethernet or coaxial cable is installed in houses, IEEE 802.3 or MoCA can collaborate with IEEE P1905.1. This hybrid technology allows new devices to access the network easily, maintains strong security, enhances the network coverage, and manages the network attentively.

First of all, IEEE P1905.1 maintains reliable connections because it adopts any possible medium. Therefore, even if a link is disconnected, it is possible to use an alternative route. Moreover, it is possible to maximize throughput with simultaneous connections. As it evenly distributes video traffic according to medium channel conditions, data congestion is also prevented. Self-network monitoring is established for uninterrupted operation.

In order to connect IEEE P1905.1 with other home network technologies, Abstraction Layer is located between the Logical Link Control (LLC) L2 layer and underlying MAC layers. The Abstraction Layer of IEEE P1905.1 abstracts PHY and MAC features of the other home network technologies using a virtual MAC. The Abstraction Layer of P1905.1 forwards Service Access Points (SAP) to the upper layers. ALME_SAP and MAC_SAP are exported for the control and data plane respectively. A layer between the LLC and MAC_SAPs of P1905.1 follows MAC/PHY Standards. In addition, The Abstraction Layer can transfer the control messages to other neighborhood Abstraction Layers. 802.3 MAC protocol data units (MDPUs) and Logical Link Control Data Units (LLCDUs) are also exchanged through P1905.1 Abstraction Layer.

3.3 Access Mechanism

3.3.1 Requirement Analysis

In order to develop a new multimedia MAC protocol for high-speed powerline communication, we considered following requirements. Starting with the QoS supporting mechanism of HomePlug 1.0 MAC for powerline communication, we considered the limitation of transmittable frame time at one time like TXOPLimit of IEEE 802.11e when the network has higher traffic load. The length of waiting queue and the number of frames waiting for its transmission in a queue are also considered for the same priority traffic in order to minimize the transmission delay so this is constrained under the threshold value.

3.3.2 Operation Principle of Voice Frame Transmission

As a highest traffic, the voice frames are transmitted with the same operation mechanism as that of HomePlug 1.0 MAC.

3.3.3 Operation Principle of Video Frame Transmission

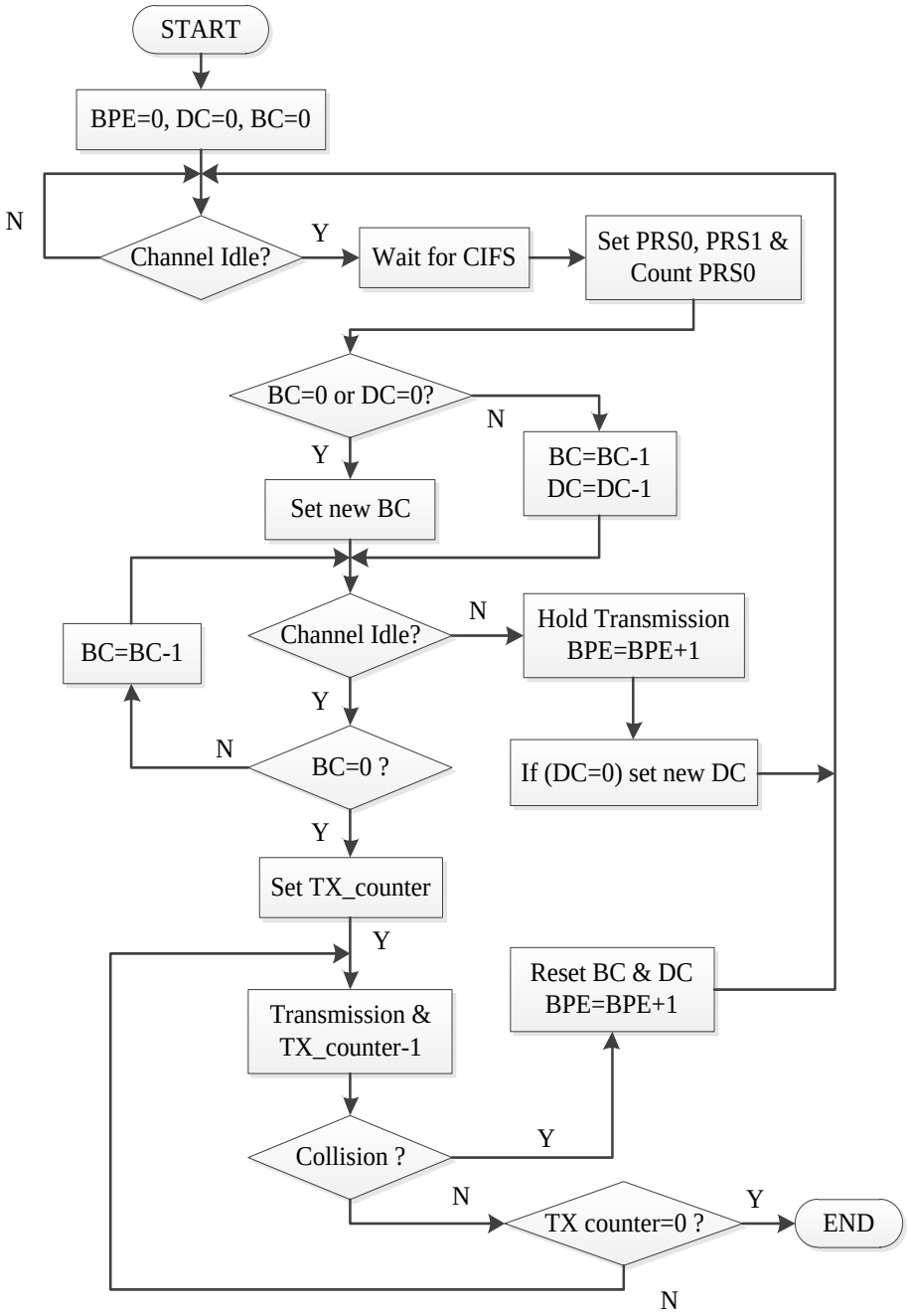

Figure 3-4. Operation principle of video transmission

When the BC is set, consider CW based on the [Buffer_Size] parameter:

- Not using fixed range CW, but using dynamic range CW based on the length of waiting queue.
- Video node having longer waiting queue will have higher transmission priority by choosing a BC from smaller range CW.
- Backoff and transmission based on the CSMA/CA.

Based on the Buffer Size, TXOP is also considered:

- TXOP: Transmittable Frame Time at one time.
- Video node having TX opportunity can transmit frames consecutively during a certain time interval based on the length of own waiting queue.

Figure. 3-4 shows the operation flow chart of our proposed mechanism for video frame transmission.

3.3.4 Operation Principle of Data Frame Transmission

When setting the BC, consider CW based on the [Buffer_Size] parameter:

- Considering TXOP based on both length of waiting queue and consecutive PRS0 count.
- When PRS0_Count is over a certain threshold, a comparatively smaller TXOP will be assigned to data nodes based on the length of their waiting queue in order to minimize the delay of multimedia traffic because it means there are many frames of multimedia traffic on the network.
- When PRS0_Count is below a certain threshold, a comparatively larger TXOP will be assigned to data nodes based on the length of their waiting queue in order to maximize the network throughput.

PRS0_Count means a parameter having consecutive number of PRS0. A data node can know how many frames of multimedia traffic (higher priority traffic) is on the network by using this parameter.

3.4 Simulation Results

In order to compare the performance between the access mechanism of HomePlug 1.0 and our proposed mechanism, we used the Network Simulator which is NS2. We developed the

simulator of our proposed mechanism from the modification of HomePlug 1.0 library module supported by NS2. Table 3-1 shows simulation parameters we considered. These parameters are based on the reference paper related to the IEEE 802.11e [2].

Table 3-1. Simulation parameters for proposed MAC algorithm

Parameter\Type	Voice	Video	Data
Inter-arrival time	Constant (0.02)	Exponential (0.01)	Exponential (0.012)
Frame size(Byte)	92	1464	1500
On time(msec)	Always	0.012	Always
Off time(msec)	0	0.088	0
Data Rate(Mbps)	0.3688	1.4	1.0

In order to simulate the powerline communication environment we considered the bus topology where 20 nodes are connected to the bus. Among them 10 nodes are for transmission only, and the other 10 nodes are for receiving. We have changed the number of transmission and receiving nodes from 2 to 10 and compared the results. The structure of each node is shown in Figure. 3-5. Each node has 4 classes of CA, and each CA has a transmission queue:

- CA3, CA2 – Multimedia Information (Voice, Video).
- CA1, CA0 – Best Effort and Background Data.

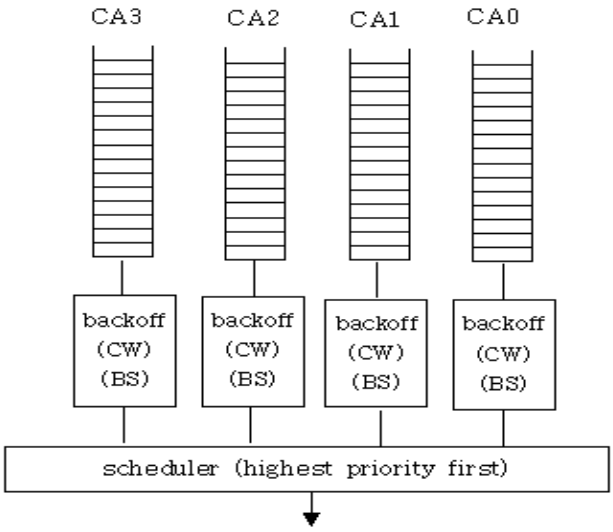

Figure 3-5. Node structure of proposed mechanism

Table 3-2. Contention window sizes and TX_counter with queue size

BPE / Queue_Size	CW				TX_count
	0	1	2	3	
0 ~ 9	7	15	15	31	1
10 ~ 15	7	15	15	31	2
16 ~ 20	3	7	15	31	3

The basic parameters we considered are the same as the HomePlug 1.0. Additionally we used the following relationship among CW, TX_count, and Queue_Size parameters as shown in Table 3-2. As the number of nodes is increased, the network throughput of our proposed mechanism shows higher performance than HomePlug 1.0 in the case of video traffic. Figure 3-6. is the comparison of video, voice, and data with the proposed scheme and HomePlug. The data rates shown are average MAC rate. When the number of nodes on a same channel is more than 3, video data throughput of proposed mechanism is better than that of typical HomePlug 1.0. However, the throughput of data traffic has nearly the same throughput characteristics between two mechanisms. Therefore, our proposed mechanism is strong for video traffic.

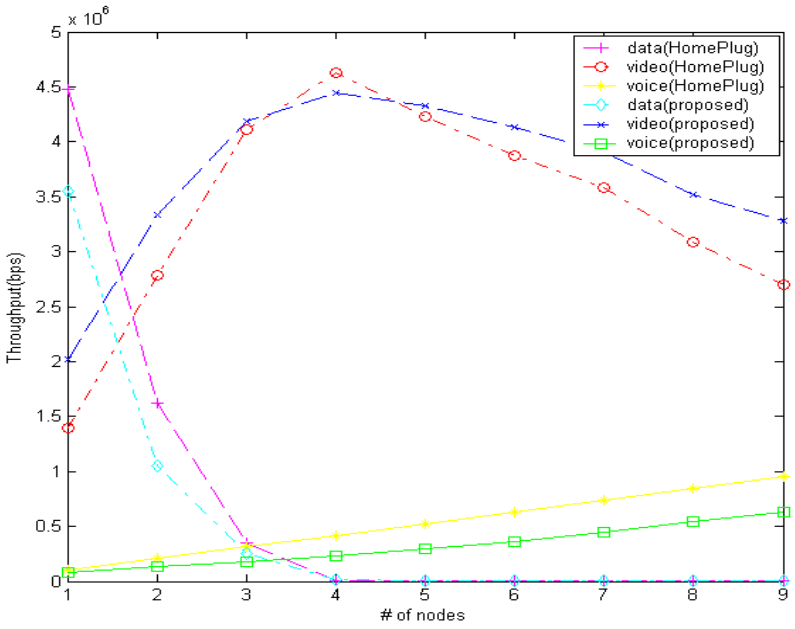

Figure 3-6. Comparison of throughput characteristics

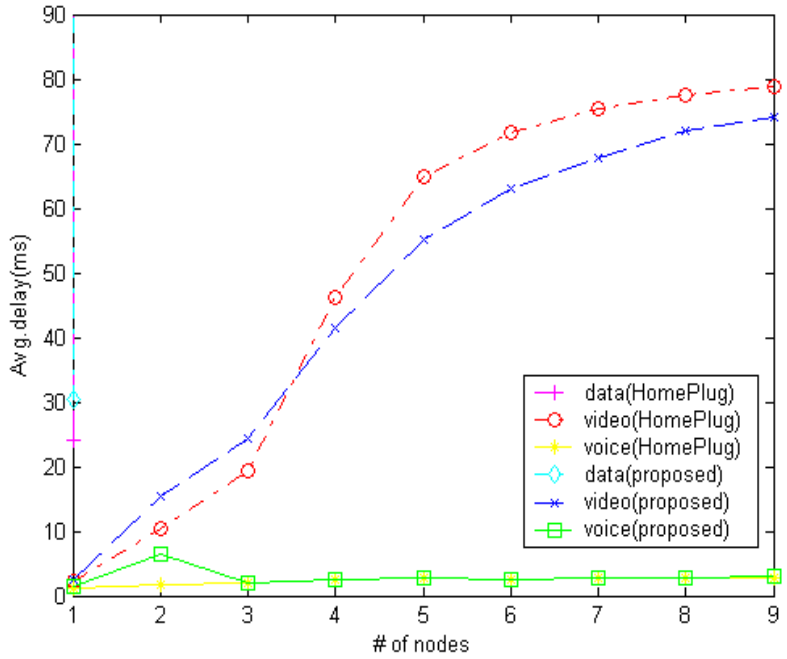

Figure 3-7. Comparison of delay characteristics

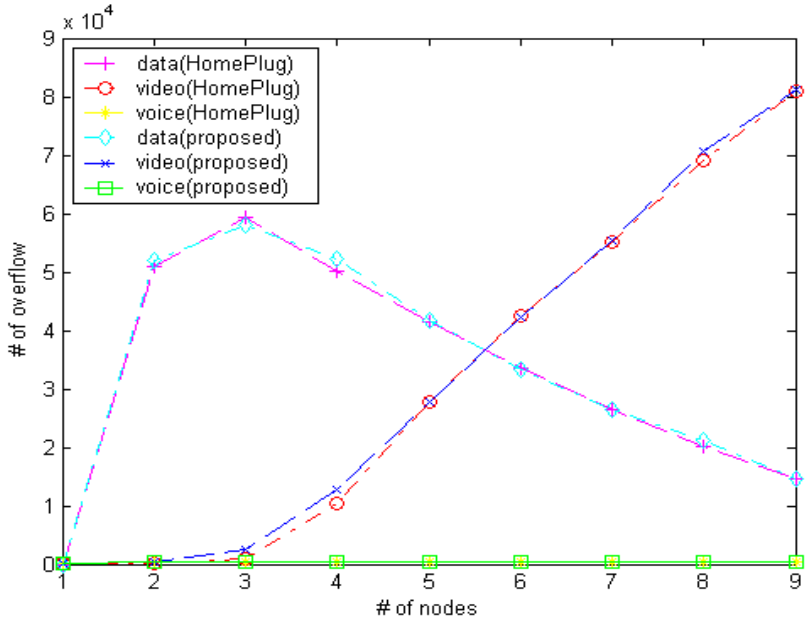

Figure 3-8. Comparison of overflow characteristics

In case of video traffic the proposed mechanism has lower average delay characteristics than HomePlug 1.0 without degradation of average delay of voice traffic. The time delay

comparison is in Figure. 3-7. During this simulation when the delay of voice and video frame exceeds the threshold values, 30ms for voice traffic and 90ms for video traffic respectively, we considered it as overflow frame and discarded it to calculate the average delay because the long delayed frame is not useful anymore. Both schemes have similar overflow characteristics as shown in Figure. 3-8. However, in case of the video traffic the proposed mechanism has about 5% lower overflow rate than HomePlug 1.0 as the number of nodes increases.

3.5 Conclusions

In Chapter 3, we proposed a new multimedia MAC protocol for high speed powerline communication. The proposed model is only focused on video traffic in order to guarantee high speed multimedia QoS. It is basically based on the HomePlug 1.0 with the addition of the TXOPLimit parameter which is a special feature in IEEE 802.11e specification. The most important parameter we added to the proposed mechanism is the length of the waiting queue for multimedia traffic. We also considered the number of waiting frames for video traffic and the number of higher priority traffic nodes for data traffic in order to decide the access priority and the range of CW in addition to the parameters for multimedia traffic for IEEE 802.11e. Simulation results show that our proposed mechanism has higher video throughput, and lower video delay without the increase of voice and data delay. In addition, the frame drop rate of data traffic according to the limited buffer size is reduced.

We will further study the HomePlug AV and IEEE P1905.1 specification to compare with our proposed mechanism for high speed powerline communication. Specially, IEEE P1905.1 can create s synergy effect and have many advantages because IEEE P1905.1 uses several network solutions. IEEE P1905.1 standard layer model with Abstraction Layer is shown in Figure 3-9. Because Abstraction Layer provides dynamic interface selection without any modification of underlying network standards, seamless Quality of Service (QoS) is guaranteed.

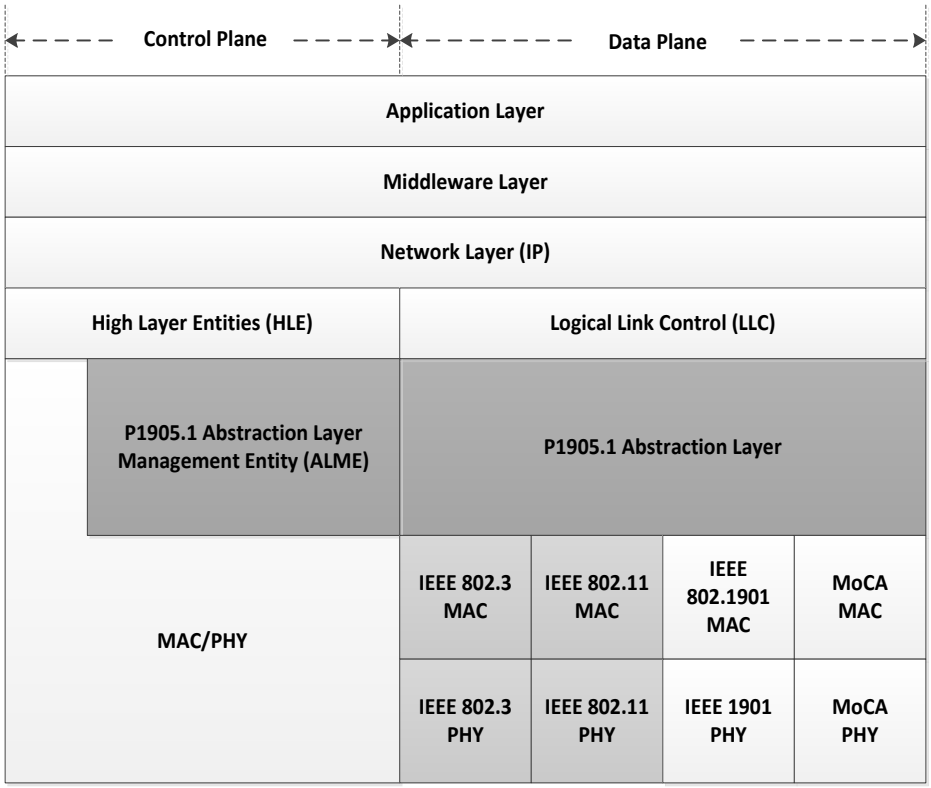

Figure 3-9. IEEE P1905.1 standard layer model

CHAPTER 4
IMPULSIVE NOISE MITIGATION ALGORITHM IN PLC

4.1 Introduction

Impulse noise, which is non-Gaussian noise is a short burst of energy and consists of single impulse or a series of impulses. Impulsive noise occurs on powerline channel frequently and degrades the performance of multi-carrier systems dramatically [4], [5]. Therefore, impulsive noise modeling and analysis are very important for channel estimation. Even if it is unpredictable and not easy to be reproduced, various impulsive noise models have been researched. The characteristics of impulsive noise in PLC systems are well studied in [6], [7], and [8]. The most common algorithms for impulsive noise detection for PLC systems perform in time domain because of computational simplicity. It is generally assumed that the impulse noise amplitudes are larger than the desired signal amplitudes for the impulsive noise detection in time domain [9]. Some algorithms perform in the frequency domain, which require additional FFT and IFFT steps [10]. Decision directed noise estimation is also one of the notable schemes but additional FFT and IFFT processes are required [41], [42].

For better performance and higher data rate, impulsive noise should be cancelled. Therefore diverse algorithms and modulation schemes have been designed to mitigate impulsive noise. Most of all, clipping methods with proper thresholds have been highly considered [11], [12]. Applying the upper and lower levels of ADC inputs is a simple method for the setting thresholds. Another way for setting the thresholds, algorithms consider the average power of received signal. The second scheme generally performs better even if it needs more memory and computations.

The goal of this work is to obtain a new impulsive noise detection threshold setting algorithm which works well in various cases of impulsive noise on PLC networks. In [43], an

iterative impulsive noise detection threshold setting algorithm was proposed and shown to outperform competing techniques. However the parameters in [43] were chosen by off-line simulation using some particular impulsive noise sources and thus the algorithm is not well suited for application to general PLC impulsive noise sources. Towards this end, we develop a general or universal impulse noise detection algorithm, with the detection threshold mathematically computed using the actual characteristics of impulsive noise in PLC systems.

The remainder of Chapter 4 is organized as follows. Impulsive noise modeling for PLC channel is in Section 4.2. The newly proposed threshold setting algorithm for impulsive noise detection is described in Section 4.3. Then, we present the detection rule to declare the location of impulsive noise samples. Simulation results are shown in Section 4.4 where we also explain the characteristics of the typical impulsive noise present in PLC networks, and finally, Section 4.5 is the conclusions.

4.2 Channel with AWGN and Impulsive Noise

For the channel deign, frequency attenuations and narrowband notches should be considered in powerline channel. We can represent impulsive response of channel as a sum of weighted delta function for multi path model.

$$h(\tau;t) = \sum_{p=0}^{N_p-1} \alpha_p(t) \cdot \delta(\tau - \tau_p(t)) \tag{4.1}$$

where N_p is the number of p th path, α_p is the channel attenuation coefficient of p th path, and τ_p is the p th delay.

The impulsive noise cause burst errors of data transmission in high frequency band. In this simulation, the Middleton's Class A model is designed in order to generate impulsive noise.

The probability density function of Middleton's Class A model is

$$f_x(x) = e^{-A}\sum_{m=0}^{\infty}\frac{A^m}{m!\sqrt{2\pi\sigma_m^2}}e^{-\frac{x^2}{2\sigma_m^2}} \tag{4.2}$$

where $\sigma_m^2 = \dfrac{\dfrac{m}{A}+\Gamma}{1+\Gamma}$, $\Gamma = \dfrac{X_G^2}{X_P^2}$

σ_m^2 is noise variance, $A = \nu_t \cdot T_s$ is impulsive index, ν_t is mean impulsive rate, and T_s is mean impulsive duration [6], [7]. Eq. 4.2 is composed of a weighted sum of Gaussian distribution. If we increase impulsive index A, the noise distribution is closed to Gaussian process, and decrease A, it is closed to Poisson process. As we can see Eq. 4.2, Γ is the ratio of powers between the Gaussian and Poisson components. This distribution with $\Gamma = 0.01$ is shown in Figure. 4.1.

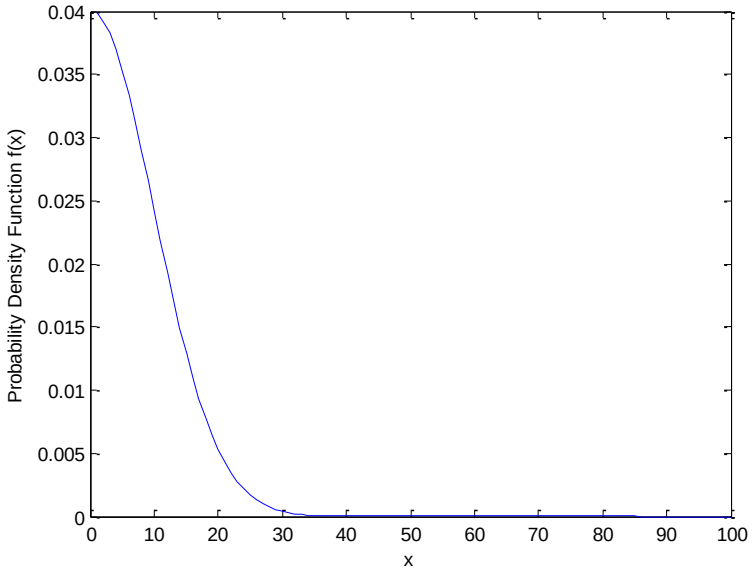

Figure 4-1. PDF of Middleton's class A model

With this Middleton's Class A model, impulsive noise can be generated such as Figure 4-2 and Figure 4-3. Middleton's Class model is a statistical and physical model to generate impulsive noise and exceedingly similar to real noise pattern. Depending on the channel condition, Γ varies. In the normal condition, for example not many electrical appliances are connected to same circuit and the circuit is stable, impulsive noise pattern would be shown such

as Figure. 4.2 ($\Gamma = 0.001$). If there are many appliances go in and out frequently to same circuit, much impulsive noise would be shown like Figure. 4.3 ($\Gamma = 0.01$).

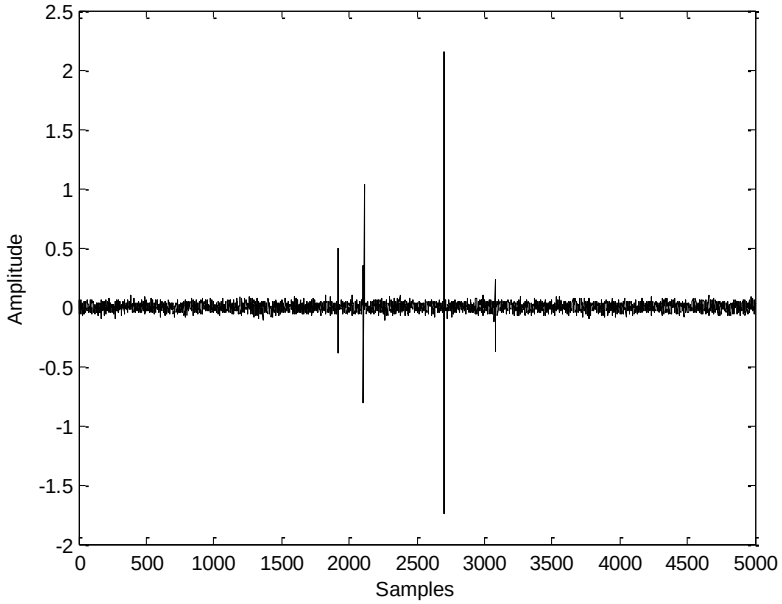

Figure 4-2. An impulsive noise example with Middleton's class A model ($\Gamma = 0.001$)

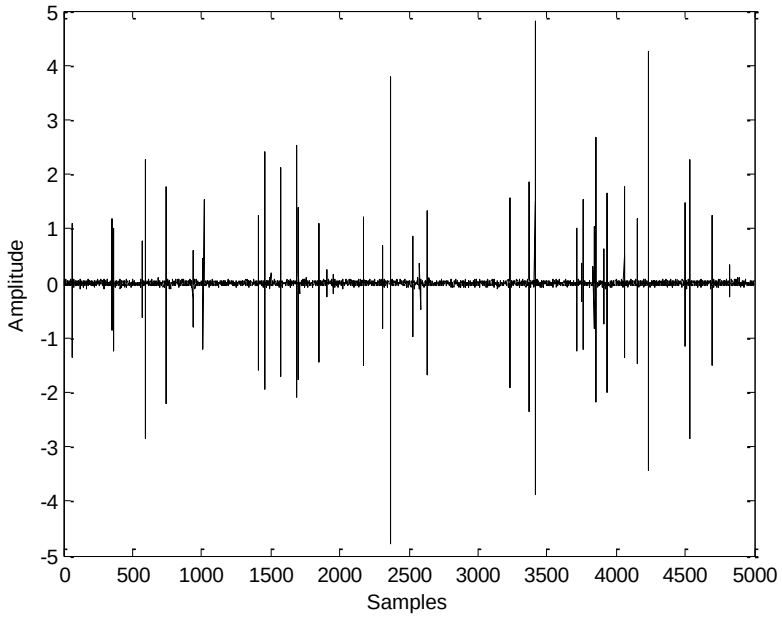

Figure 4-3. An impulsive noise example with Middleton's class A model ($\Gamma = 0.01$)

4.3 Threshold Setting Algorithm for Impulsive Noise Detection

For the impulsive noise mitigation, exact impulsive noise detection process should be preceded. Therefore, we propose a new threshold setting algorithm in Section 4.3. It is important to decide a proper threshold values to identify desired signal from impulsive noise. Generally, the magnitude of impulsive noise is larger than the maximum magnitude of the desired signal. We define the peak of the desired signal as the ideal detection threshold value. The proposed algorithm operates to find the close value of the ideal detection threshold. The received signal on time domain can be represented as

$$y(t) = h(t) * x(t) + n(t) + i(t) \tag{4.3}$$

where h(t), x(t), n(t), and i(t) are channel response, transmit signal, Gaussian noise, and impulsive noise respectively. We assumed that a single impulsive noise consists of constant and exponential term $e^{-t/\tau}$. Then, impulsive noise pulse on time domain can be defined as

$$I(t) = |i(t)| = \alpha_{MAX} e^{-kt} \tag{4.4}$$

where k and α_{MAX} represent a damping factor and the possible peak value of impulsive noise, respectively. The magnitude of the impulsive noise pulse at a certain time T can be represented as

$$I(T) = \alpha = \alpha_{MAX} e^{-kT} \tag{4.5}$$

Then, the instant time T can be represented as

$$T = -\frac{1}{k} \ln \frac{\alpha}{\alpha_{MAX}} \tag{4.6}$$

The energy of impulsive noise between 0 to T can be represented as

$$P = \int_0^T \alpha_{MAX} e^{-kt} dt = \frac{\alpha_{MAX}}{k} \left[1 - e^{-kT} \right] \tag{4.7}$$

Substituting T in Eq. 4.6 for Eq. 4.7, we can obtain

$$P = \frac{\alpha_{MAX}}{k}\left[1 - \frac{\alpha}{\alpha_{MAX}}\right] \tag{4.8}$$

We assume that we know the ideal threshold α_{IDEAL}. From Eq. 4.8, the damping factor k can be expressed as

$$k = \frac{\alpha_{MAX}}{P_I}\left[1 - \frac{\alpha_{IDEAL}}{\alpha_{MAX}}\right] \tag{4.9}$$

P_I is the integration of impulsive waveform envelope larger than the ideal threshold. Substituting for k in Eq. 4.8 from Eq. 4.9, P can be expressed as

$$P = P_I \frac{\alpha_{MAX} - \alpha}{\alpha_{MAX} - \alpha_{IDEAL}} \tag{4.10}$$

Using Eq. 4.4, the ideal threshold α_{Ideal} can be obtained

$$\alpha_{IDEAL} = \alpha_{MAX} e^{-kt_{IDEAL}} \tag{4.11}$$

where t_{IDEAL} is defined as the time instant for the ideal threshold. Using Eq. 4.7, P_I can be represented as

$$P_I = \frac{\alpha_{MAX}}{k}\left[1 - e^{kt_{IDEAL}}\right] \tag{4.12}$$

Then, the time instant t_{IDEAL} can be represented as

$$t_{IDEAL} = -\frac{1}{k}\ln\left[1 - \frac{P_I k}{\alpha_{MAX}}\right] \tag{4.13}$$

Substituting Eq. 4.13 into Eq. 4.4, the ideal threshold can be represented as

$$\begin{aligned}\alpha_{IDEAL} &= \alpha_{MAX} e^{-kt_{IDEAL}} \\ &= \alpha_{MAX}\left[1 - \frac{P_I k}{\alpha_{MAX}}\right]\end{aligned}$$

$$= \alpha_{MAX} - P_I k \tag{4.14}$$

As we can see the Eq. 4.3, the received signal consists of the impulsive noise $i(t)$ and other components. In order to separate the impulsive noise from the desired signal, the mean of the absolute value of signal envelope is adopted. A_y, A_i and A_x are defined as the absolute value means of waveform envelope for the received signal, impulsive noise samples, and the others components respectively. Then, the relationship between signals is $A_y = A_x + A_i$, and AWGN is ignored. Moreover, R is the peak to average ratio of the absolute value of the transmit signal envelope. Because $n(t)$ is ignored, the ideal threshold can be represented as $\alpha_{IDEAL} = R \cdot A_x$.

Manipulating Eq. 4.10, P_I can be represented as

$$P_I = P\frac{\alpha_{MAX} - RA_x}{\alpha_{MAX} - \alpha} = P\left[1 + \frac{RA_i}{\alpha_{MAX} - \alpha}\right] \tag{4.15}$$

where $A_i = P_I / L$ and L is the block size for impulsive noise detection procedure. Then, P_I can be represented as

$$P_I = \frac{(\alpha_{MAX} - \alpha)PL}{(\alpha_{MAX} - \alpha)L - PR} \tag{4.16}$$

If the ideal threshold is not available, the damping factor value is not known in Eq. 4.9. Instead, α_{IDEAL} is substituted for α as the alternative value in Eq. 4.9 then

$$\tilde{k} = \frac{\alpha_{MAX}}{P_I}\left[1 - \frac{\alpha_{THRE}}{\alpha_{MAX}}\right] \tag{4.17}$$

Finally, the new impulsive noise detection threshold is possible to represent as

$$\alpha_{THRE} = \alpha_{MAX} - P_I \tilde{k} \tag{4.18}$$

Once the threshold is set, the following step is the process to find impulse noise locations. Figure 4.4. is the flow chart to define start and stop points of impulsive noise. Shift register R

with a length M is adopted to find starting point. If the received signal amplitude is larger than or equal to the threshold α , the shift register R(1) become 1 and the register shifts at the time instant t. When the sum of the shift registers is larger than the impulse staring point threshold N, our algorithm considers this point as a starting point of the impulse noise. If 15 samples from the impulse starting point are larger than or equal to the threshold value, the impulse map $I_{map}(t)$ is set to be one. The same process to find impulsive noise location restarts after 15 samples from last impulsive noise detected.

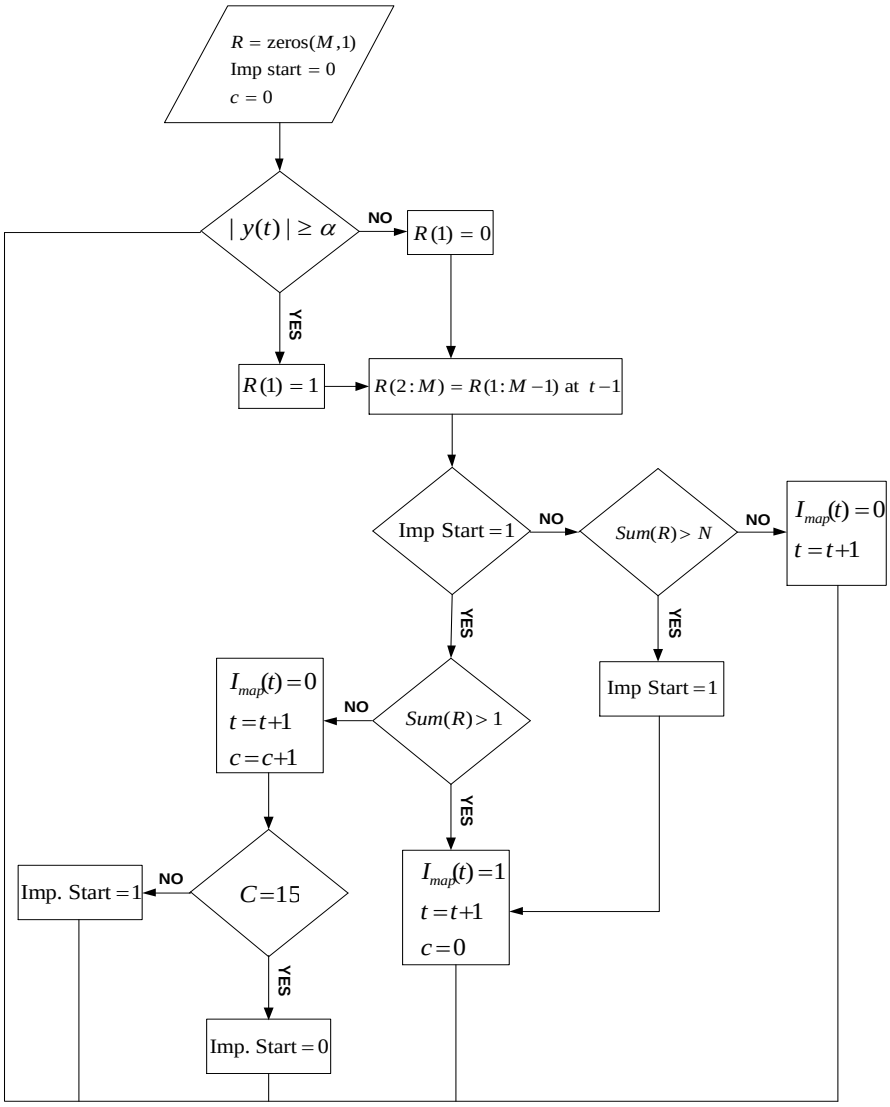

Figure 4-4. Impulsive noise detection flow chart

4.4 Simulation Results

Four threshold values are compared in Section 4.4. α_{IDEAL} is the ideal threshold which is the maximum magnitude of the signal without impulse noise. α_{ROUGH} represents the rough threshold which is obtained by conventional envelope threshold method. α_{OLD} is obtained with the threshold which is previously proposed in [43]. α_{NEW} is the threshold of the proposed threshold setting algorithm from Section 4.3. In our previous work, we obtained proper parameter values for good performance and use same parameters for this simulation. According to previous reference, an impulse starting point threshold *N* is assigned to 1, the shift register length *M* is 8, and *C* is 15 [43]. We generate impulsive noise sequences using the statistical model presented in Section 4.2. Because this noise model adopts a stochastic distribution approximation based on noise measurements, it is similar to a real impulsive noise channel and is widely used.

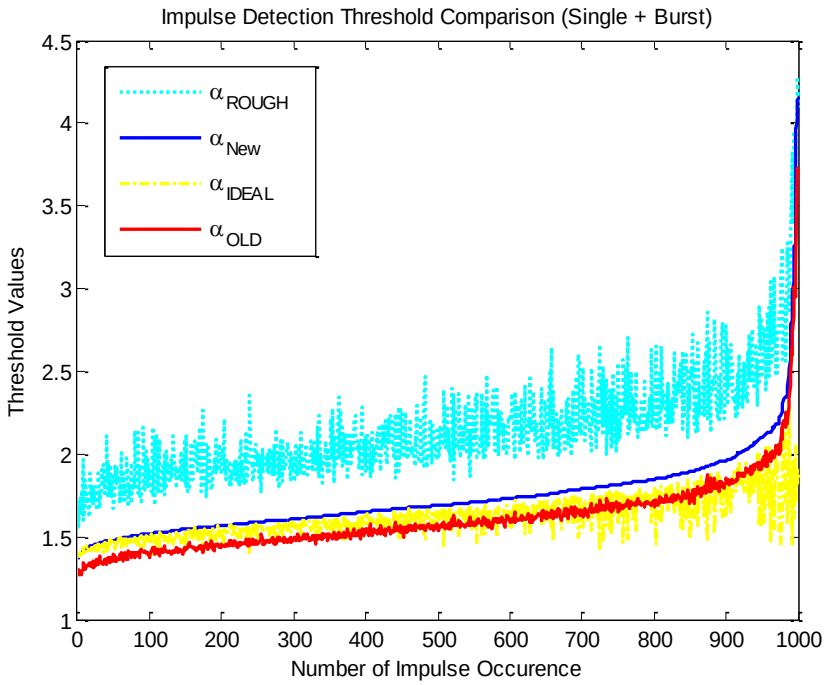

Figure 4-5. Performance comparison of impulsive detection algorithms

Figure 4.5 shows the performance comparison of impulsive detection algorithms with a combination of single impulses and bursts of impulsive noise. Because the result of rough threshold shows a significant gap with the ideal threshold, it is impossible to detect impulsive noise properly with conventional threshold method. As we can see Figure 4.5, the threshold values of α_{OLD} and α_{NEW} are very close to α_{IDEAL}. Even, the threshold values of α_{OLD} are sometimes closer to α_{IDEAL} than α_{NEW}. However, the values of α_{OLD} is smaller than α_{IDEAL} generally so it is possible to consider the desired signal as impulsive noise. In this case, we call it false detection. However, the false detection rate of α_{NEW} is much less than α_{OLD} because the threshold values of α_{NEW} are larger than α_{IDEAL} in most cases. Therefore, α_{NEW} is more desirable to detect impulsive noise correctly. Table 4-1 is the comparison of the false detection rates between our previously algorithm and the newly proposed algorithm. The newly proposed algorithm outperforms the previously proposed algorithm at all impulsive noise types.

Table 4-1. False impulse detection threshold rate (%)

Impulse Noise Type	$\alpha_{IDEAL} > \alpha_{NEW}$	$\alpha_{IDEAL} > \alpha_{OLD}$
Single	2.2	30.1
Burst	2.1	73
Single + Burst	1.8	51.2

4.5 Conclusions

In Chapter 4, new threshold setting algorithm is proposed for the impulsive noise detection and performs better than conventional and previously proposed algorithms. The new proposed algorithm not only finds thresholds close to the ideal threshold, but false impulse detection rate is low significantly. Therefore, impulsive noise can be detected correctly with the newly proposed algorithm, and then it is mitigated with clipping method.

CHAPTER 5
ERROR CONTROL CODES WITH ADAPTIVE MULTI-CARRIER OFDM FOR PLC CHANNEL

5.1 Introduction

The error correcting performance of LDPC and turbo codes is closed to Shannon limit. Therefore, both codes outperform other error correcting codes with relatively lower complexity. In order to find and choose proper error coding scheme, we compare LDPC and turbo codes with previous research works. The encoding process of LDPC codes is complex and decoding process is simple comparatively. However, encoding process of turbo codes is simple and decoding process is complex. As the code length is extended, the complexity is exponentially increased.

LDPC codes tend to show better performance at higher code rate. However, turbo codes generally works better at lower code rates. The notable applications and standards of LDPC codes are G.hn, DVB-S2, high speed Ethernet, and optional part of IEEE 802.11n. Turbo codes are adopted at DVB-RCS, IEEE 802.16, and 3G and 4G mobile telephone standard such as HSPA, EV-DO, and LTE.

There are previous research comparisons of LDPC and turbo codes under various standard and channel conditions. In [44], BER with rate 1/3 turbo code is better than BER with (7200,4797) regular LDPC code on AWGN environment. However, LDPC codes work better than turbo codes on a typical cyclostionary Gaussian process environment. In order to compare FEC schemes on ITU-T , high-level metrics, Iteration and Memory Comparison Factor (ICF and MCF) are proposed [45]. QC-LDPC for ITU-T outperforms Convolutional Turbo Code (CTC) at the result. LDPC and turbo codes are compared with receiver diversity on AWGN channel [46]. Two error correcting codes are compared with various number of receiver diversity. LDPC codes exhibit less BER than turbo codes with same receiver diversity scheme at all scenarios. Packet error rate (PER) and decoding complexity of rate compatible LDPC and turbo codes are

compared in the OFDM with Evolved UTRA downlink which is the radio interface of Long Term Evolution (LTE) [47]. At the simulation result, turbo codes are more reliable than LDPC codes because similar PER and decoder complexity are shown between LDPC and turbo Codes. The advantage and disadvantage of LDPC and turbo codes on satellite interactive system are researched [48]. The common construction method for LDPC codes with 1/2 code rate is also introduced. In order to mitigate the high Peak to Average Power Ratio (PAPR) of MIMO-OFDM scheme on 4G mobile systems, error correcting codes are applied such as LDPC, turbo, and concatenated Turbo-Reed Solomon codes [49]. LDPC codes outperform the other coding methods at simulation.

The remainder of Chapter 5 is organized as follows. Section 5.2 represents DMT system and adaptive modulation with examples of simulation results. The theoretical and mathematical analysis of LDPC and turbo codes is described in Section 5.3 and 5.4. The simulation results with comparison of LDPC and turbo codes are in Section 5.5. Then, Section 5.6 is the conclusion of Chapter 5.

5.2 DMT System with Adaptive Modulation

DMT system is an application of OFDM with efficient bit-loading scheme. In order to improve data rate with limited SNR, adaptive modulation with multi-carrier OFDM is designed in Chapter 5. Specially, channel estimation is preceded for adaptive modulation and impulsive noise.

Block diagram of a transceiver with DMT system is shown in Figure. 5-1. First, the analog signal is converted into discrete and parallel signal for modulation. According to the channel condition, each subcarrier of OFDM uses different modulation schemes. Information bits per carrier also vary from 0 bit to 15 bits, which depend on modulation schemes. HomePlug AV specification [26] adopted BPSK, QPSK, 8-QAM, 16-QAM, 256-QAM, and 1024-QAM

modulation schemes with maximum 10 bits, but we adopt 15 bits to increase the maximum bits. The reason of this try is that maximum 15 bits, which is from 0 to 15 so 16 possible levels, are the power of 2. Therefore, this scheme can diminish redundancy and make system efficient. If the 15 bits adaptive QAM modulation is realized with affordable error rate, data rate is possible to be improved.

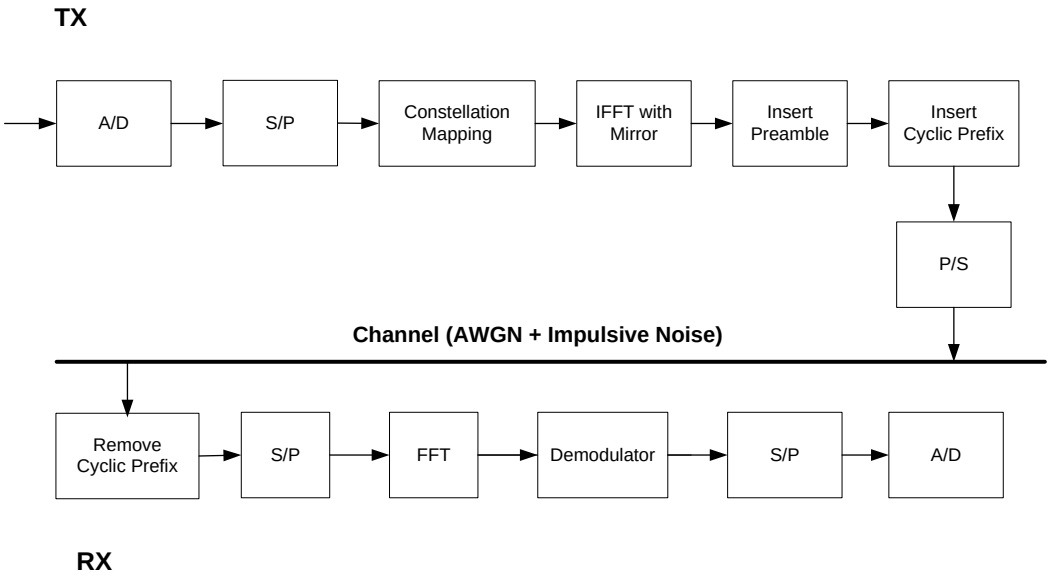

Figure 5-1. The block diagram of transceiver with DMT OFDM system

The number of transmission frequency subchannel could be power of two, and we assume 256 subchannels, which is common number for DMT system [50]. Since noise power is not same at spread bandwidth, we can assign different data bits to each subchannel. The SNR for each channel is given by

$$SNR_i = \frac{\varepsilon_i \left| H_i \right|^2}{\sigma_i^2} \tag{5.1}$$

where ε_i and $\left| H_i \right|^2$ are the signal energy and the power spectral density of i th channel.

The bits per each channel is given by

$$b_i = \frac{1}{2}\log_2\left(1+\frac{SNR_i}{\Gamma}\right) \tag{5.2}$$

where Γ is the SNR gap, which means how far the system is from the maximum achievable capacity. Therefore, the total number of bits, sum of each channel bits is

$$b = \sum_{i=1}^{N} b_i = \frac{1}{2}\sum_{i=1}^{N}\log_2\left(1+\frac{SNR_i}{\Gamma}\right) \tag{5.3}$$

According to dividing total number of bits with the symbol duration T, we can obtain bit rate B and can express as

$$B = \frac{1}{T}b = \frac{1}{T}\cdot\frac{1}{2}\sum_{i=1}^{N}\log_2\left(1+\frac{SNR_i}{\Gamma}\right) \tag{5.4}$$

$\max_{E_i} b = \frac{1}{2}\sum_{i=1}^{N}\log_2\left(1+\frac{\varepsilon_i \cdot g_i}{\Gamma}\right)$, $\varepsilon = \sum_{i=1}^{N}\varepsilon_i$, $g_i = |H_i|^2 / \sigma_i^2$, $\varepsilon_i + \frac{\Gamma}{g_i} = \text{constant}$ [50].

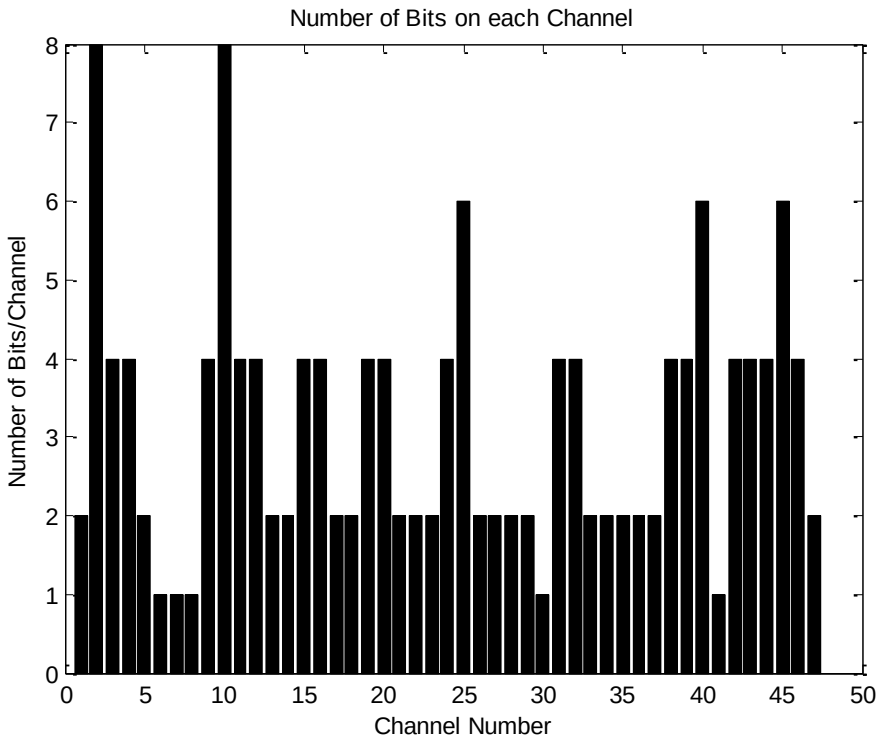

Figure 5-2. Number of bits on each subchannel with DMT OFDM system

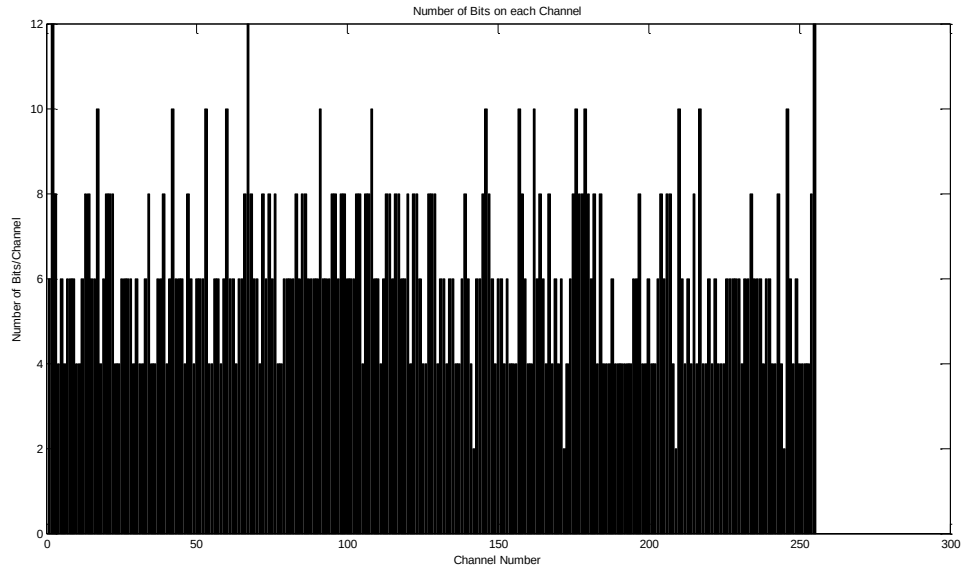

Figure 5-3. An example of DMT OFDM system

Figure. 5-2 and Figure. 5-3 are examples for the number of bits on each channel with DMT OFDM system. Depending on each channel condition, the number of assigned bits is different. Because assigned bits on each subchannel are different, adaptive modulation scheme is applied. This modulation scheme is based on QAM, but we can carry variable information bits. Since the maximum number of bits on a subchannel is 15, it is possible to carry 2^{15} information bits of data. More bits can be assigned to subchannels with DMT than regular OFDM.

5.3 Low Density Parity Check (LDPC) Codes

LDPC codes are linear block codes obtained from sparse bipartite grapes. LDPC codes are first designed by Gallager, and perform near Shannon limit which is the theoretical maximum for a symmetric memory less channel.

Sparse parity check matrix $\boldsymbol{H}$ of LDPC codes have mostly 0's and few 1's. It is

$$\boldsymbol{v} \cdot \boldsymbol{H}^T = 0 \tag{5.5}$$

where codeword $\boldsymbol{v} = (v_1, v_2, v_3, \ldots, v_n)$.

The codeword is generated by $k \times n$ generate matrix $\boldsymbol{G}$,

$$\boldsymbol{v} = \boldsymbol{uG} \tag{5.6}$$

where $\boldsymbol{v} = (v_1, v_2, v_3, \ldots, v_n)$.

5.3.1 Regular and Irregular LDPC Codes

A regular LDPC codes contain same number of 1's in each column, w_c, and same number of 1's in each row, $w_r = w_c(n/m)$. The following matrix $\boldsymbol{H}$ is an example of sparse parity check matrix for regular (10,5) LDPC code with w_c =2 and w_r =4. Each column of $\boldsymbol{H}$ means a coded bit and each row is a parity check sum [51].

$$H = \begin{bmatrix} 1 & 1 & 1 & 1 & 0 & 0 & 0 & 0 & 0 & 0 \\ 1 & 0 & 0 & 0 & 1 & 1 & 1 & 0 & 0 & 0 \\ 0 & 1 & 0 & 0 & 1 & 0 & 0 & 1 & 1 & 0 \\ 0 & 0 & 1 & 0 & 0 & 1 & 0 & 1 & 0 & 1 \\ 0 & 0 & 0 & 1 & 0 & 0 & 1 & 0 & 1 & 1 \end{bmatrix} \tag{5.7}$$

Tanner designed LDPC codes with a proposed graphical representation method which is Tanner graph. Tanner graph can express the decoding process of LDPC codes effectively and completely. Figure. 5-4 is an example of Tanner graph with (10,5) LDPC code and it can describe a parity check matrix $\boldsymbol{H}$ intuitively in Eq. 5.7. Tanner graph has two different nodes which are the variable nodes (v-node) and the check nodes (c-node). Each row of a parity check matrix $\boldsymbol{H}$ is to match each check node of Tanner graph, and each column of a parity check matrix $\boldsymbol{H}$ is to match each variable node of Tanner graph. Check node *i* is connected to neighbor variable node *j* when h_{ij} in $\boldsymbol{H}$ is assigned to 1. Otherwise, it is not connected, the value of this element is 0. Therefore, n variable nodes and m=n-k check nodes are existed in a parity check matrix $\boldsymbol{H}$ and are matched to Tanner graph.

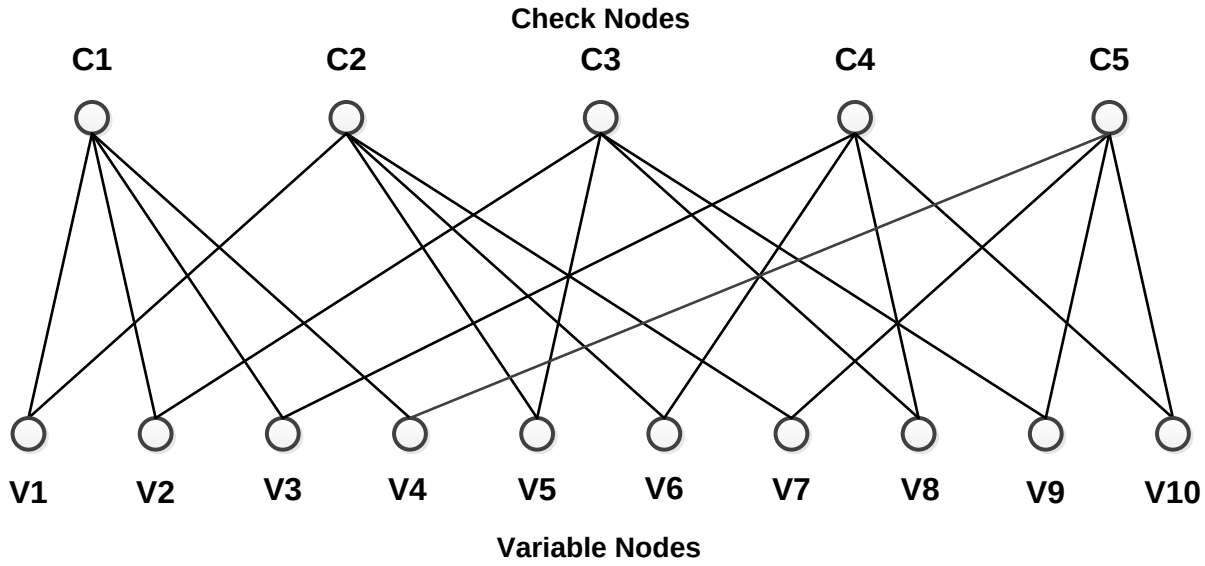

Figure 5-4. An example of tanner graph for LDPC code

On the other hand, irregular codes consist of different number of 1's in each column and row. Therfore, parameter w_c and w_r are assigned with various values at each column and row. $\lambda(x)$ which is the v-node degree distribution polynomial is represented as

$$\lambda(x) = \sum_{d=1}^{d_v} \lambda_d x^{d-1} \tag{5.8}$$

where λ_d means the fraction of all edges which is connected to variable nodes with degree d, and d_v is the maximum degree of variable node.

$\rho(x)$ which is the c-node degree distribution polynomial is represented as

$$\rho(x) = \sum_{d=1}^{d_c} \rho_d x^{d-1} \tag{5.9}$$

where ρ_d means the fraction of all edges which is connected to check nodes with degree d, and d_c is the maximum degree of check node [51].

5.3.2 Iterative Decoding Algorithm

For the decoding preocess of LDPC codes, iterative decoding algorithms is suitable to update check node and variable node information. Gallager proposed a optimal decoding algorithm, sum-product algorithm, based on the idea of belif propagation [14]. Sum-product algorithm operates iteratively to calculate and update check node and variable information. For the decision, a posteriori probability (APP) is applied for decoding that each bit in the transmiitted codeword $\boldsymbol{v} = (v_1, v_2, v_3, \ldots, v_n)$ is 1 with the received word $\boldsymbol{y} = (y_1, y_2, y_3, \ldots, y_n)$. The APP ratio is the likelihood ratio such as

$$l(v_j \,|\, \boldsymbol{y}) = \frac{P(v_j = 0 \,|\, \boldsymbol{y})}{P(v_j = 1 \,|\, \boldsymbol{y})} \tag{5.10}$$

In order to obtain practical results, Log Likelihood Ratio (LLR) is widly used because it is a numerically stable algorithm. LLR is represented as

$$L(v_j \,|\, \boldsymbol{y}) = \log\left(\frac{P(v_j = 0 \,|\, \boldsymbol{y})}{P(v_j = 1 \,|\, \boldsymbol{y})} \right) \tag{5.11}$$

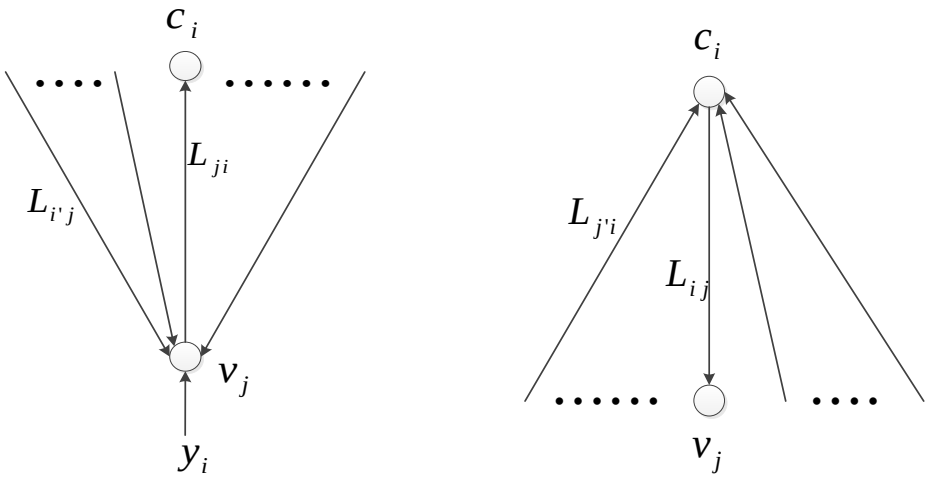

(a) A variable Node Decoder (b) A Check Node Decoder

Figure 5-5. Sum-product algorithm process for LDPC decoding

Two figures in Figure. 5-5 shows the iterative process of sum-product algorithm for LDPC decoding. Figure. 5.5 (a) is a variable node decoder which consists of a repetation decoder. The information of v_j, a variable node *j*, is updated after it collects information bits from received signal y_j and connected neighbor check nodes except c_i. After v_j, a variable node *j* computes and updates information based on received data, v_j send a extransic information, L_{ji}, to check node c_i. A check node decoder process in Figure. 5-5 (b) is also similar. After c_i, a check node *i* receives and updates LLR information from neighbor variable nodes except v_j, calculated information L_{ij} sends to v_j.

For the exact estimation of decoding process, variable decoders and check node decoders operate iteratively and cooperatively. The operation is stopped when the assigned maxium number of iterration is reached or the system considers that all errors are corrected . Based on the Gallager sum-product algorithm [14], the outgoing variable node information from c_i to v_j is represented as

$$L_{ij} = 2\tanh^{-1}\left(\prod_{j'\in N(i)-\{j\}} \tanh\left(\frac{1}{2}L_{j'i}\right)\right) \tag{5.12}$$

The extrinsic information from v_j to c_i

$$L_{ji} = L_j + \sum_{i'\in V_j\backslash i} L_{i'j} \tag{5.13}$$

After the last iteraion, v_j estimates the received information based on

$$L_j^{tot} = L_j + \sum_{i\in V_j} L_{ij} \tag{5.14}$$

Finally, $\hat{v}_i = 1$, when $L_j^{tot} < 0$, and $\hat{v}_i = 0$, when $L_j^{tot} > 0$.

5.4 Turbo Codes

Because of the high performance of turbo codes, it is widely used for FEC method. There are two structures of turbo codes which are Parallel and Serial Concatenated Convolutional Codes (PCCCs and SCCCs). Basically the turbo encoder is configured with two or more convolutional encoders connected with pseudo-random interleavers. For the decoding process, the iterative soft decision algorithm is mainly adopted. HomePlug AV standard also applied turbo code for FEC.

5.4.1 Encoder

Figure. 5-6 is an example of Parallel Concatenated Convolution Code (PCCC) for turbo encoder [51]. It is configured with two Recursive Systematic Convolutional (RSC) encoders with N bit pseudo-random interleaver. Two identical RSC codes operate generally. The generator matrix of turbo codes are represented as

$$G(D) = \left[1 \quad \frac{g^{(2)}(D)}{g^{(1)}(D)} \right] \tag{5.15}$$

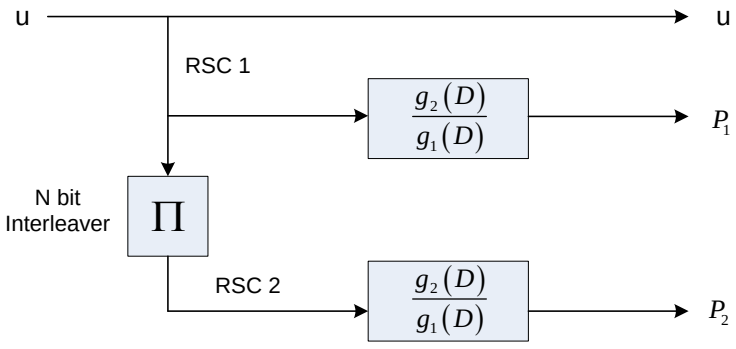

Figure 5-6. Basic configuration of turbo encoder

When input sequence is divisible by $g^{(1)}(D)$, the code sequence with input and the generator, $u(D)G(D)$, is finite. The pseudo-random interleaver, which is a permuter, rearranges

the input data for encoder 2. Because a puncturer transmits two parity information P_1 and P_2 alternately, the rate 1/3 encoder works as a rate 1/2 code. In order to decrease coding overhead, the puncturer punctures P_1 and P_2 alternately.

5.4.2 Decoder

The turbo decoder is shown in Figure. 5-7. Two iterative decoders cooperate to estimate and correct received signal. Maximum a posteriori probability (MAP) algorithm for soft decision is the basic structure of the decoder. Decoder 1 decodes with received original bits x' and first parity bits p'_1 from first encoder. Decoder 2 decodes with permutated original bits and second parity bits p'_2 from second encoder. After soft decision at each decoder, bits $L_e^1(x)$ from decoder 1 and $L_e^2(x)$ from decoder 2 enter opposite decoders for the iterative decoding process.

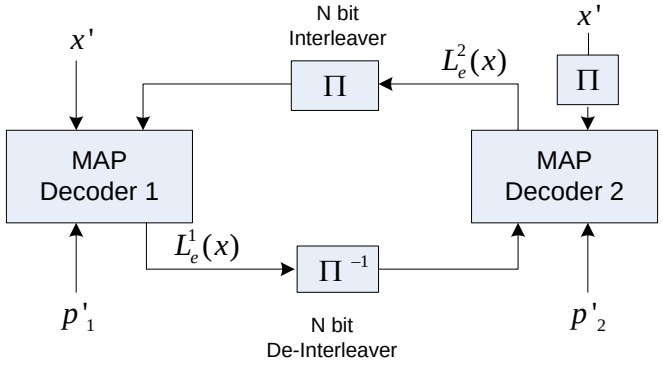

Figure 5-7. Basic configuration of turbo decoder

BCJR algorithm concept is applied for the MAP decoding process of turbo codes. The Log a Posteriori Probability (LAPP) ratio for modified BCJR algorithm can be represented as

$$L(u_k) = \log\left(\frac{P(u_k = +1|y)}{P(u_k = -1|y)}\right) \tag{5.16}$$

With the code's trellis, we can represent

$$L(u_k) = \log\left(\frac{\sum_{S^+} P(s_{k-1} = s', s_k = s, y)/P(y)}{\sum_{S^-} P(s_{k-1} = s', s_k = s, y)/P(y)}\right) \tag{5.17}$$

Therefore, the modified BCJR-MAP algorithm is shown in below.

$$L(u_k) = \log\left(\frac{\sum_{S^+} \tilde{\alpha}_{k-1}(s') \cdot \gamma_k(s', s) \cdot \tilde{\beta}_k(s)}{\sum_{S^-} \tilde{\alpha}_{k-1}(s') \cdot \gamma_k(s', s) \cdot \tilde{\beta}_k(s)}\right) \tag{5.18}$$

where $\alpha_k(s) = p(s_k = s, y_1^k)$, $\beta_k(s) = p(y_{k+1}^N | s_k = s)$, and $\gamma_k(s', s) = p(s_k = s, y_k | s_{k-1} = s')$.

MAP decoder with LAPP ratio can be also represented as

$$L(u_k) = \log\left(\frac{P(y|u_k = +1)}{P(y|u_k = -1)}\right) + \log\left(\frac{P(u_k = +1)}{P(u_k = -1)}\right) \tag{5.19}$$

where the second equation is a priori information. In typical case, it is zero because

$P(u_k = +1) = P(u_k = -1)$

However, decoder 1 and decoder 2 exchange extrinsic information iteratively. It is possible to be expressed as

$$L(u_k) = \log\left(\frac{\sum_{S^+} \tilde{\alpha}_{k-1}(s') \cdot \gamma_k^e(s', s) \cdot C_k}{\sum_{S^-} \tilde{\alpha}_{k-1}(s') \cdot \gamma_k^e(s', s) \cdot C_k}\right)$$

$$= L_c y_k^s + L^e(u_k) + \log\left(\frac{\sum_{S^+} \tilde{\alpha}_{k-1}(s') \cdot \gamma_k^e(s', s) \cdot \tilde{\beta}_k(s)}{\sum_{S^-} \tilde{\alpha}_{k-1}(s') \cdot \gamma_k^e(s', s) \cdot \tilde{\beta}_k(s)}\right) \tag{5.20}$$

where $C_k = \exp\left[\frac{1}{2} u_k \left(L^e(u_k) + L_c y_k^s\right)\right]$

Decoder 1 computes $L_1(u_k) = L_c y_k^s + L_{21}^e(u_k) + L_{12}^e(u_k)$ and $L_{12}^e(u_k)$ is extrinsic information passed from decoder 2 to decoder 1 [51].

5.5 Simulation Results and Comparison

In order to compare the performance of uncoded, turbo, and LDPC codes, the simulation is implemented. In this work, we have considered AWGN and impulsive noise channel using the Middleton's class A model. OFDM with discrete multitone scheme is adopted for adaptive modulation. In order to find better performance, various code rates and sizes are applied. At the receiver, the procedure is reverse process of transmitter.

In this simulation, various block sizes of LDPC codes are applied from (128,64) to (1024,512). These matrices are randomly generated based on sparse bipartite grapes. For the sparsity of weights in LDPC codes, $w_c = 1$, $w_c = 2$, $w_c = 4$, and $w_c = 8$ are assigned for (128,64), (256,128), (512, 256), and (1024,512) LDPC codes. Maximum iteration number is set to 10 so parity check repetition for error correction performs up to 10 times. For the turbo code simulation, we adopted rate 1/3 puncturing encoder and maximum a posteriori probability (MAP) algorithm with soft decision for decoder. Frame size is decided to 1024 and iteration is also 10.

Figure. 5-8 represents bits error rates of uncoded system and LDPC codes with 128, 256, and 1024 codeword. Because we fixed the code rate with 1/2 in this simulation, parity check bits are 64, 128, and 512 respectively. As we can see the Figure. 5.7, error rates of LDPC codes using lager block size outperform than LDPC codes with smaller block size.

The comparison of uncoded, LDPC, and turbo codes are shown in Figure. 5-8, Figure. 5-9, and Table 5-1. Various block sizes are adopted for LDPC simulation same as previous simulation. Turbo code performs better than other LDPC codes when SNR is less than 3 dB. However, LDPC codes with large block size such as N=1024 outperform the turbo code when SNR is 3 dB or more. As we can see in those results, LDPC codes with larger block size improve the bit error rates.

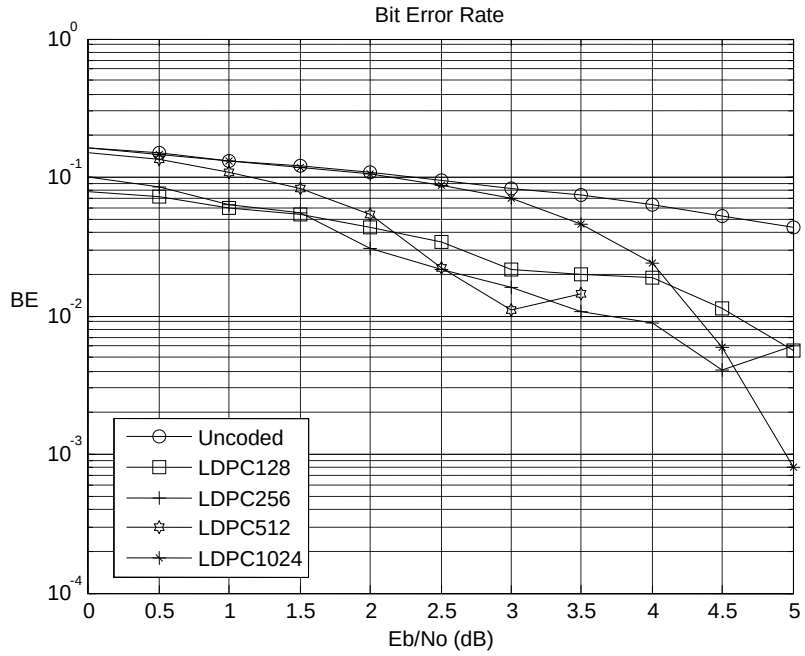

Figure 5-8. Bit error rates of uncoded and LDPC codes

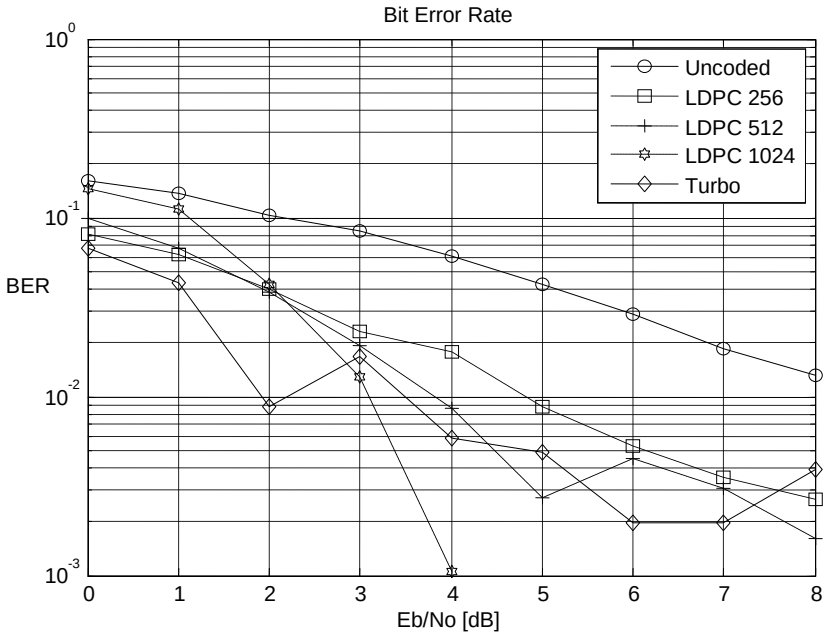

Figure 5-9. Bit error rates of uncoded, LDPC, and turbo codes

Table 5-1. Bit error rates of uncoded, LDPC, and turbo codes

	0	1	2	3	4	5	6	7	8
Uncoded	0.1622	0.1357	0.1040	0.0839	0.0606	0.0421	0.0289	0.0186	0.0130
LDPC 256	0.0813	0.0625	0.0400	0.0231	0.0178	0.0088	0.0053	0.0035	0.0026
LDPC 512	0.0983	0.0668	0.0384	0.0194	0.0086	0.0027	0.0045	0.0030	0.0016
LDPC 1024	0.1466	0.1112	0.0426	0.0128	0.0011	0	0	0	0
Turbo	0.0674	0.0430	0.0088	0.0166	0.0059	0.0049	0.0020	0.0020	0.0039

5.6 Conclusions

In Chapter 5, LDPC codes with turbo codes were compared on PLC channel. For the modulation, DMT system with adaptive modulation scheme is adopted. During the LDPC codes simulation, we attempted to apply several LDPC code rate. LDPC codes results show better performance at higher code rate generally.

CHAPTER 6
QUASI-CYCLIC (QC) LDPC CODES ON REAL PLC CHANNEL AND G.HN STANDARD

6.1 Introduction

A Quasi-Cyclic (QC) code is one of the linear block codes over GF(2). A (tb,k) QC code C_{qc} depend on positive integers b, k, and t with the constraint k < tb. There are two conditions to generate a QC code. First, each codeword should consist of t sections with b bits each. In addition, every codeword after a cyclic shift in C_{qc} should be a codeword in C_{qc} [51]. In order to advance the FEC performance for PLC, we design and propose new LDPC codes based on a Quasi-Cyclic form with various code rates and block sizes.

Several QC-LDPC codes have been introduced previously. In order to design efficient QC-LDPC codes with better minimum distance, two methods based on finite geometries or circulant permutation matrixes are generally applied [52], [53], and [54].

The parity-check matrices of the proposed QC-LDPC codes are generated with circulant permutation matrices which consist of arrays of circulants. We can obtain circulant permutation matrices after column permutation process using a permutation matrix. The main advantage of QC-LDPC codes compared with random LDPC codes is that the encoding procedure involves easier implementation and simpler structure. Furthermore, memory requirement is significantly reduced than randomly generated LDPC codes.

The remainder of Chapter 6 is organized as follows. Section 6.2 represents the encoding procedure with theoretical and mathematical analysis of QC-LDPC. Two decoding processes are described in Section 6.3. Simulation results with comparison of QC-LDPC codes are represented in Section 6.4. For the simulation, G.hn standard with real PLC channel noise is adopted. Then, Section 6.5 is the conclusion of Chapter 6.

6.2 Encoding Process for QC-LDPC Codes

In Section 6.2, we introduce a parity check matrix H for QC-LDPC encoding. A parity check matrix H is configured with square block matrices which are either circulant permutation matrices or the zero matrices. Circulant permutation matrices are generated by the permutations of a base matrix P, called a permutation matrix. The following matrix is an example of permutation matrix P which is square block with size $q \times q$.

$$P = \begin{bmatrix} 0 & 1 & 0 & \cdots & 0 \\ 0 & 0 & 1 & \cdots & 0 \\ \vdots & \vdots & \vdots & & \vdots \\ 0 & 0 & 0 & \cdots & 1 \\ 1 & 0 & 0 & \cdots & 0 \end{bmatrix} \tag{6.1}$$

In order to generate parity check matrix H of QC-LDPC codes, a permutation process is performed with a cyclic shift. Therefore, circulant permutation matrix P^i is generated from the identity matrix I with i times right shift ($0 \le i \le q$) and P^∞ is defined as the zero matrix. The parity check matrix H of QC-LDPC code is composed of circulant permutation matrices. Eq. 6.2 denotes a parity check matrix H of QC-LDPC code.

$$H = \begin{bmatrix} P^{a_{11}} & P^{a_{12}} & \cdots & P^{a_{1(k-1)}} & P^{a_{1k}} \\ P^{a_{21}} & P^{a_{22}} & \cdots & P^{a_{2(k-1)}} & P^{a_{2k}} \\ \vdots & \vdots & \vdots & \vdots & \vdots \\ P^{a_{j1}} & P^{a_{j2}} & \cdots & P^{a_{j(k-1)}} & P^{a_{jk}} \end{bmatrix} \tag{6.2}$$

where $a_{il} \in \{0,1,...,q-1,\infty\}$.

The size of H is $(j \cdot q) \times (k \cdot q)$ and overall code rate is R ≥ 1 – j / k. The parameter q should be a prime number and the size of k satisfies $j \le k \le q$ for proper encoding. After the locations of

parameters in the first row are decided, the other parameters of each block matrix P follow the first row schedule. Therefore, the memory storage requirement can be reduced.

The parity check matrices of regular and irregular QC-LDPC codes are generated with following the rule denoted below. Generally irregular QC-LDPC codes outperform regular codes because some bit nodes are connected to a large number of check nodes relatively, which means some of information bits are possible to correct values faster. Regular and irregular QC-LDPC code examples are in the following. Eq. 6.3 is a parity check matrix example of an array code for QC-LDPC codes.

$$H(q,j)=\begin{bmatrix} I & I & I & \cdots & I \\ I & P & P^2 & \cdots & P^{q-1} \\ I & P^2 & P^4 & \cdots & P^{2(q-1)} \\ \vdots & \vdots & \vdots & \cdots & \vdots \\ I & P^{j-1} & P^{(j-1)2} & \cdots & P^{(j-1)(q-1)} \end{bmatrix} \tag{6.3}$$

The size of q is a prime number and a positive integer with $j \le q$. A (j,q) regular QC-LDPC code is generated with H(q,j) which has j ones in each column and q ones in each row. H(q,j) has rank qj-j+1 and the code rate can be defined as

$$R=\frac{q^2-qj+j-1}{q^2}=1-\frac{qj-j+1}{q^2}>1-\frac{j}{q} \tag{6.4}$$

The matrix below Eq. 6.5 is a parity check matrix of a modified array code for irregular QC-LDPC codes.

$$H(q,j,k)=\begin{bmatrix} I & I & I & \cdots & I & \cdots & I \\ 0 & I & P & \cdots & P^{(j-2)} & \cdots & P^{(k-2)} \\ 0 & 0 & I & \cdots & P^{2(j-3)} & \cdots & P^{2(k-3)} \\ \vdots & \vdots & \vdots & \cdots & \vdots & \cdots & \vdots \\ 0 & 0 & \cdots & 0 & I & \cdots & P^{(j-1)(k-j)} \end{bmatrix} \tag{6.5}$$

It is an upper triangular form which has full rank, and q is prime number with $j \le k \le q$. The overall code rate is given by

$$R = \frac{qk - qj}{qk} = \frac{k - j}{k} = 1 - \frac{j}{k} \tag{6.6}$$

QC-LDPC codes have a cycle of finite length with several constraints. A parity check matrix with the cycles of the short length decline QC-LDPC performance. Therefore, we need to optimize a block cycle for high performance. First, we define the mother matrix or base matrix M(H) which is m by n. Mother matrix M(H) generated by circulant permutation matrices in the parity check matrix given in (6.2). If a circulant permutation matrix consists of two or more block cycles, it is regarded an overlap between block cycles [55], [56].

A block cycle with length $2l$ in a parity matrix H of (6.2) can be described by the chain

$$P^{a_1} \to P^{a_2} \to \cdots \to P^{a_{2l}} \to P^{a_1} \tag{6.7}$$

where the block cycle is $2l$.

As we can see Eq. 6.2, p^{a_i} and $p^{a_{i+1}}$ are located in the same row block or the same column block of H, and p^{a_i} and $p^{a_{i+2}}$ are located in the different row or column blocks. Eq. 6.7 is the chain constraint with a $2l$ block cycle.

If r is the least positive integer then the block cycle is a cycle of length $2lr$ [56].

$$r \cdot \sum_{i=1}^{2l} (-1)^{i-1} a_i \equiv 0 \mod L \tag{6.8}$$

6.3 Decoding Process for QC-LDPC Codes

6.3.1 Sum-Product Algorithm

Sum-Product Algorithm which is Belief Propagation Algorithm is a common iterative decoding algorithm of LDPC codes. This soft decision algorithm based on bipartite graph performs better than hard decision algorithm in most cases. Several modified sum product

Algorithm schemes have been proposed in previous researches [57], [58]. The iterative sum product algorithm follows the below process. First, variable nodes collect received signal from channel, and then each variable node sends its message to connected check nodes called neighboring check nodes. The messages from neighboring variable nodes are calculated and estimated at each check node. After, all messages at check nodes are determined, these estimated messages are sent back to neighboring variable nodes. The message from a check node to a variable node is the information received from all other neighboring variable nodes except the variable node we want to send information. The process is same when it comes to messages sent from variable nodes to check nodes. The message exchange between variable nodes and check nodes with estimation is one iteration. The iteration process is repeated till the correct codeword is obtained or the predefined maximum iteration number is reached. After all iteration process is terminated, one entire codeword is estimated.

6.3.2 Bit-Flipping Algorithm

Bit-flipping algorithm is an iterative algorithm for a hard decision decoding. The decoding process consists of the following steps using parity check matrix H and vector y at each iteration. First, calculate $H \cdot y^T$ with modulo 2 additions and then check which elements of $H \cdot y^T$ equal 1. After every bit nodes resolve the number of unsatisfied check nodes, find the largest number of unsatisfied check nodes. In order to estimate correct information, modify the bits of y involving the unsatisfied check nodes. Until the maximum number of iteration or $H \cdot y^T = 0$ is satisfied, the previous processes should be iterated. During the each iteration several bits are simultaneously flipped with original bit flipping algorithm. The original algorithm is possible to flip not only incorrect bits but also correct bits. In order to prevent this

problem only one bit flipping algorithm at each iteration is proposed previously [55]. However, one bit flipping algorithm requires the more maximum number of iteration for acceptable results.

6.4 Simulation Results and Comparison

For the QC-LDPC simulation, we have applied 10 real powerline noise data which are captured at a real house. Intellon (Qualcomm Atheros) provides the real PLC channel noise for the simulation in Section 6.4. The powerline circuit is connected with home appliances such as a refrigerator, TVs, electric lamps, and PCs.

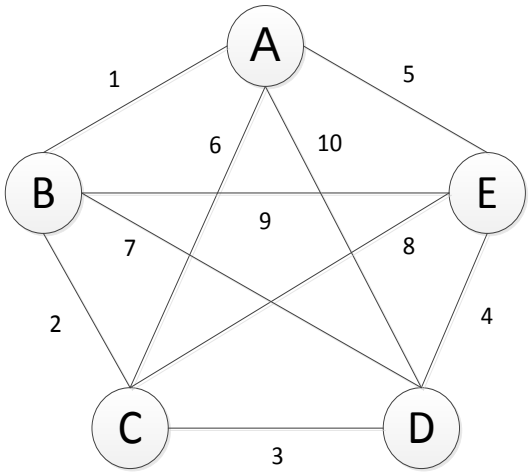

Figure 6-1. PLC network configuration with 5 nodes and 10 channels

As we can see the Figure. 6-1, 5 nodes are connected with powerline and 10 paths are configured for this simulation. Node A, B, C, D, and E are access points in a test house. We have captured frequency response and impulsive noise data of 10 channels from path 1 to 10.

Figure 6-2 and Figure 6-3 are two of 10 PLC noise data we captured. Figure 6-2-a and Figure 6-3-a are 600000 PLC noise samples from two nodes at a house. Figure. 6-2-b and Figure. 6-3-b are 10000 samples which are close looks of Figure 6-2-a and Figure 6-2-b respectively. PLC noise consists of AWGN and impulsive noise. Depending on channel condition, many different noise patterns are generated. For instance, the noise shown in Figure. 6-2 has impulsive noise with consistent period and AWGN noise. However, AWGN noise is dominant with less

impulsive noise in Figure. 6-3. In order to compare the performance of QC-LDPC codes depending on channel and noise condition, we have applied 10 different channels and noise data.

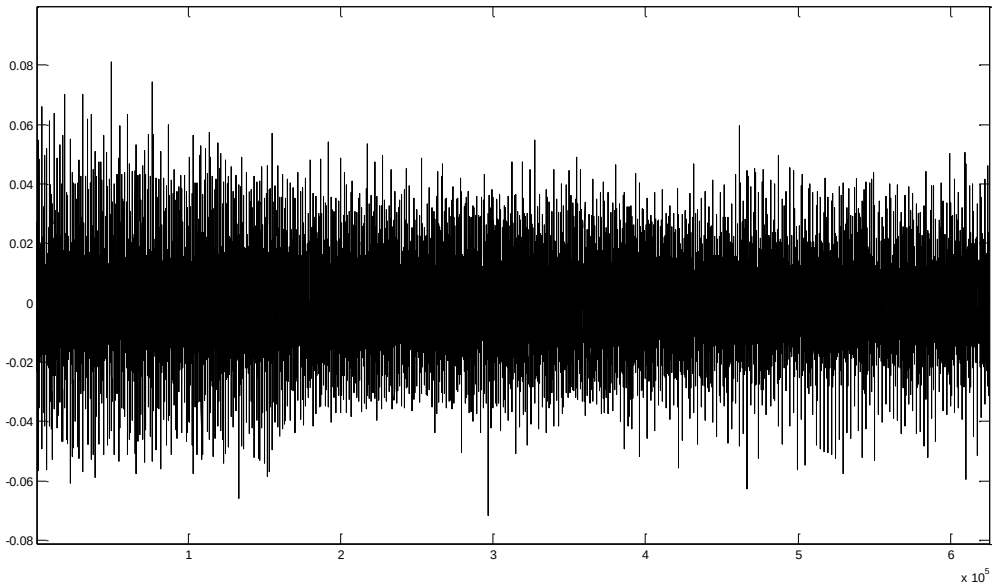

(a)

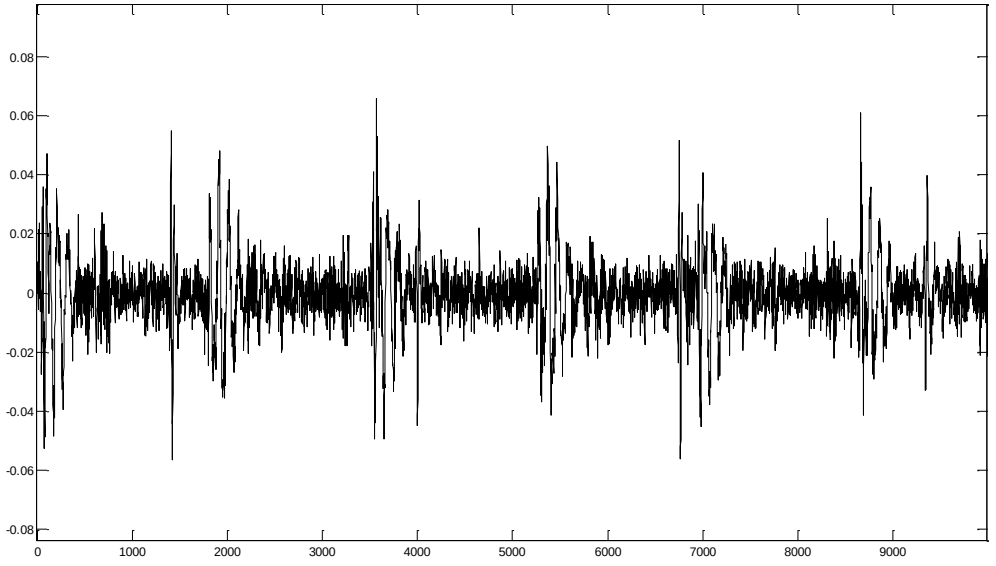

(b)

Figure 6-2. Real noise on PLC channel (a) 600000 samples (b) 10000 samples

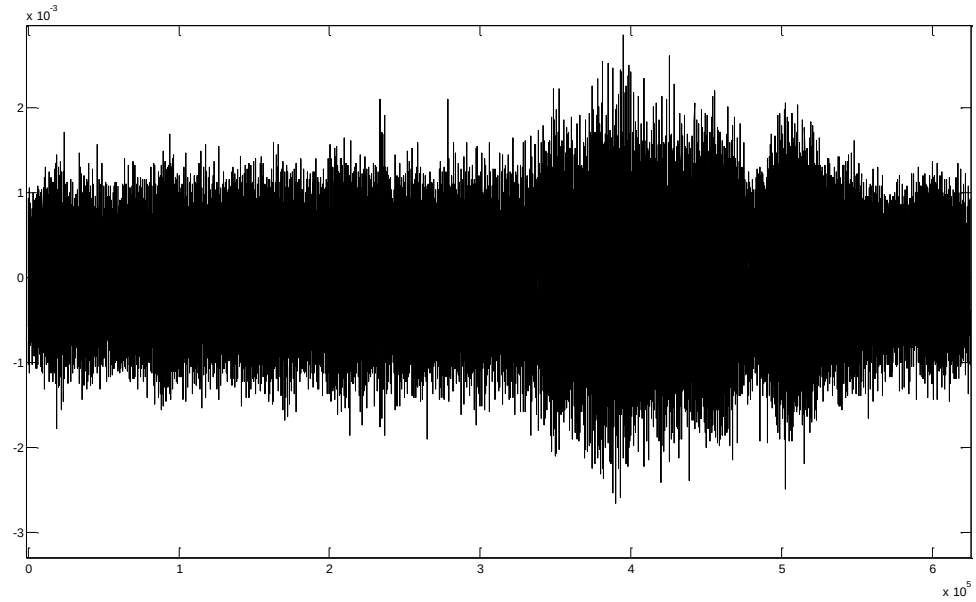

(a)

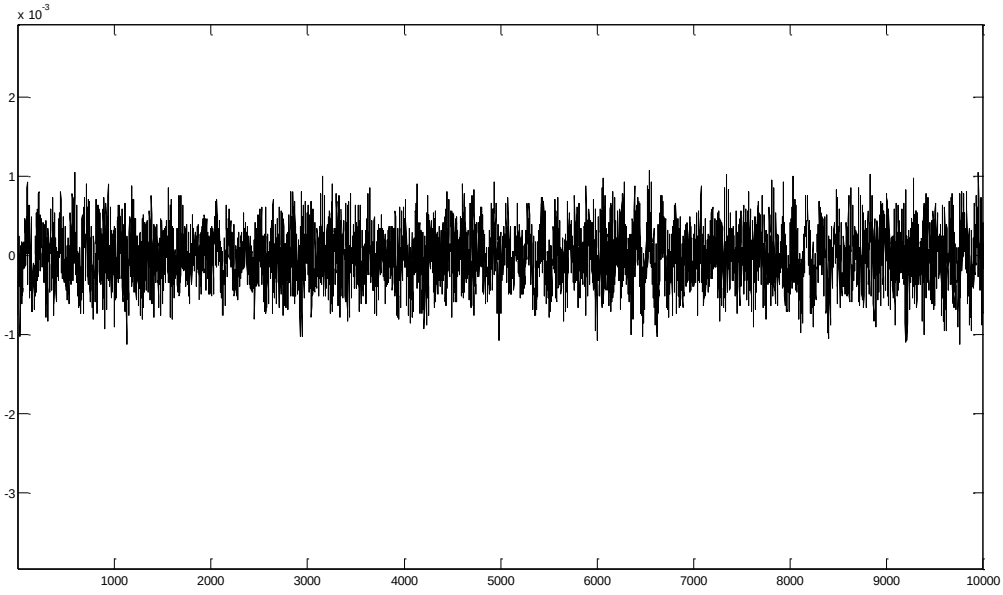

(b)

Figure 6-3. Real noise on PLC channel (a) 600000 samples (b) 10000 samples

The captured noise on real channel is adopted for the simulation in Section 6.4. The real noise in Figure 6-2 is adopted for the results of QC-LDPC comparison with different block sizes

and code rates. First, we have compared (3600,3000), (3600,2400), and (3600,1800) QC-LDPC codes which are 5/6, 2/3, and 1/2 code rates respectively. For the decoding, sum-product algorithm is applied with 10 maximum iterations. As we can see Figure 6-4, QC-LDPC codes with less code rate outperform than higher code rate codes. Less code rate means that parity bits are less relatively. Therefore, even if QC-LDPC codes with low code rate perform better, we should endure more redundant bits.

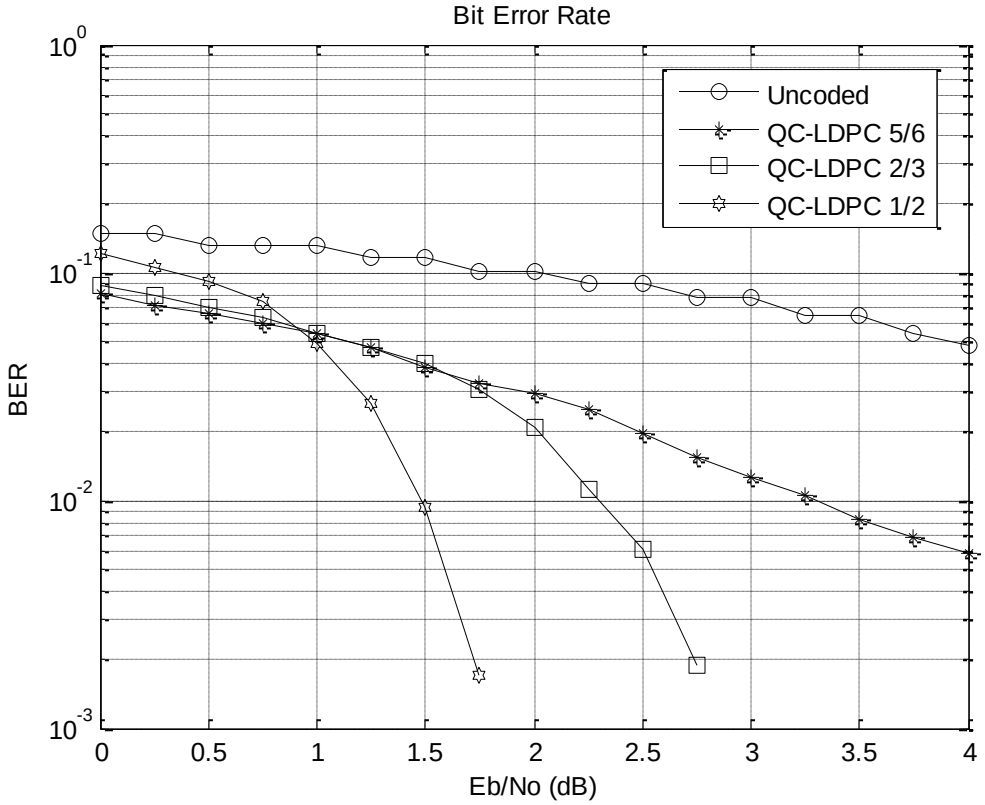

Figure 6-4. Comparison of QC-LDPC codes with different code rates (N=3600)

Table 6-1. Comparison of QC-LDPC codes with different code rates (N=3600)

	0	0.5	1	1.5	2	2.5	3	3.5	4
Uncoded	0.1489	0.1311	0.1311	0.1161	0.1017	0.0900	0.0775	0.0653	0.0475
QC-LDPC 5/6	0.0803	0.0656	0.0536	0.0381	0.0292	0.0197	0.0125	0.0083	0.0058
QC-LDPC 2/3	0.0878	0.0706	0.0544	0.0400	0.0208	0.0061	0	0	0
QC-LDPC 1/2	0.1211	0.0908	0.0492	0.0094	0	0	0	0	0

QC-LDPC codes with different block sizes are also compared in Figure 6-5. In order to compare only block sizes, we use same code rate which is 1/2. Therefore, (1800,600), (3600,1800), and (5400,2700) QC-LDPC codes are simulated. BERs of (5400,2700) QC-LDPC code are less than BERs of the other codes in most SNRs. QC-LDPC codes with large block size perform better than smaller block size codes. However, the performance was not improved significantly when the block sizes are large enough.

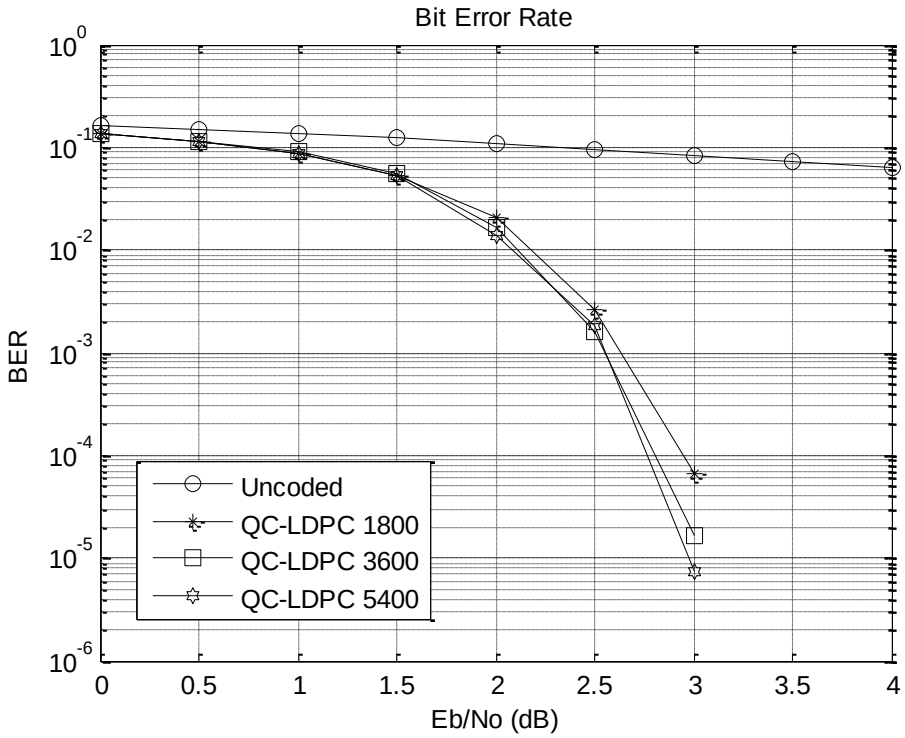

Figure 6-5. Comparison of QC-LDPC codes with different block sizes

Table 6-2. Comparison of QC-LDPC codes with different block size

	0	0.5	1	1.5	2	2.5	3	3.5	4
Uncoded	0.1624	01489	0.1344	0.1222	0.1080	0.0963	0.0845	0.0724	0.0625
QC-LDPC 1800	0.1375	0.1142	0.0887	0.0560	0.0162	0.0016	0.0006	0	0
QC-LDPC 3600	0.1362	0.1142	0.0887	0.0560	0.0162	0.0016	0.0001	0	0
QC-LDPC 5400	0.1388	0.1151	0.0873	0.0535	0.0140	0.0015	0	0	0

Moreover, QC-LDPC codes of G.hn standard are compared with real noise. G.hn standard adopted 7 different LDPC codes with different sizes and rates for forward error

correction of header and payload information [30]. We applied 3 different QC-LDPC codes with large block sizes for payload information in our simulation. Table 6 shows QC-LDPC standard for G.hn. Bit error rates are compared with three different block size codes using different code rates.

Table 6-3. G.hn standard for QC-LDPC

	Codeword size	Information bits	Parity bits	Code rate
QC-LDPC 5184	5184	4320	864	5/6
QC-LDPC 6480	6480	4320	2160	2/3
QC-LDPC 8640	8640	4320	4320	1/2

We have compared (5184,4320), (6480,4320), (8640,4320) QC- LDPC codes with code rate 5/6, 2/3, and 1/2 respectively. For the turbo code simulation, data size N=6480 with code rate 1/2 is applied. For the G.hn QC-LDPC simulation, 10 real noise channels are used. Two simulation results with real noise from Figure 6-2 and 6-3 are represented in Figure 6-6 and 6-7. As we can see the Figure 6-6 and 6-7, (8640,4320) QC_LDPC code outperforms than other codes in most SNRs. When SNR is higher than 2 dB, BERs of (8640,4320) QC-LDPC code are 0 on real noise channels. Large block size QC-LDPC code with low code rate generally shows better performance than the other codes using small block sizes with high code rates. Depending on the channel characteristics, the results are a little different. For example, turbo code works better than (5184,4320) QC-LDPC code when SNR is less than 4.5 dB in Figure 6-6. Thus, turbo code performs better than (5184,4320) QC-LDPC code of G.hn in particular SNRs and channels. However, BERs of most G.hn QC-LDPC codes are lower than BERs of turbo code predominantly. Therefore, it is important to choose a proper FEC scheme depending on channel conditions. Moreover, we need to consider appropriate code rates to escape too many redundant bits.

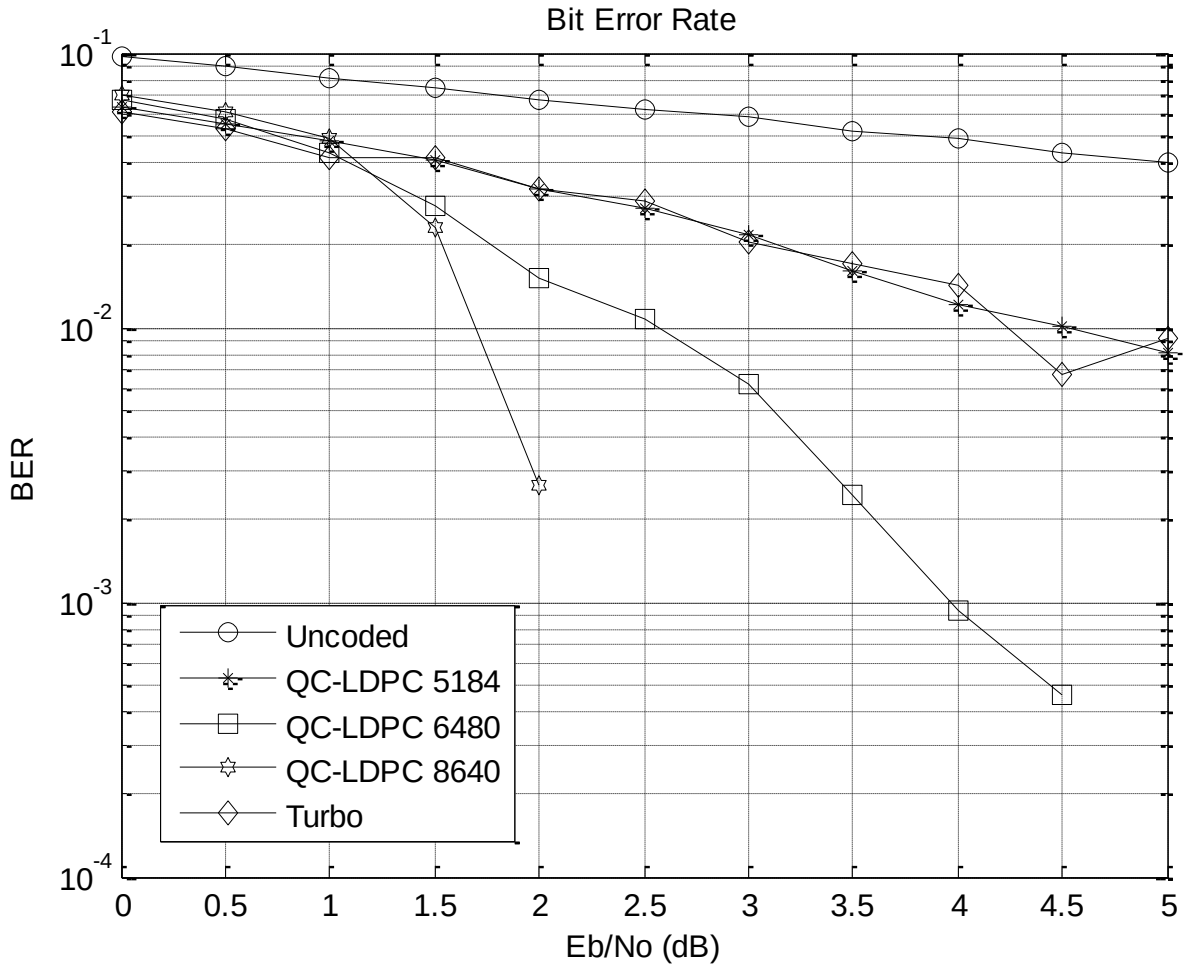

Figure 6-6. Comparison between turbo and QC-LDPC codes with G.hn standard

Table 6-4. Comparison between turbo and QC-LDPC codes with G.hn standard

	0	0.5	1	1.5	2	2.5	3	3.5	4	4.5
Uncoded	0.0968	0.0891	0.0807	0.0740	0.0681	0.0618	0.0581	0.0514	0.0490	0.0434
Turbo code	0.0605	0.0533	0.0417	0.0419	0.0319	0.0286	0.0206	0.0172	0.0144	0.0067
QC-LDPC 5184 (5/6)	0.0631	0.0550	0.0476	0.0403	0.0316	0.0270	0.0216	0.0162	0.0122	0.0100
QC-LDPC 6480 (2/3)	0.0677	0.0573	0.0435	0.0276	0.0151	0.0106	0.0062	0.0025	0.0009	0.0005
QC-LDPC 8640 (1/2)	0.0708	0.0612	0.0484	0.0233	0.0027	0	0	0	0	0

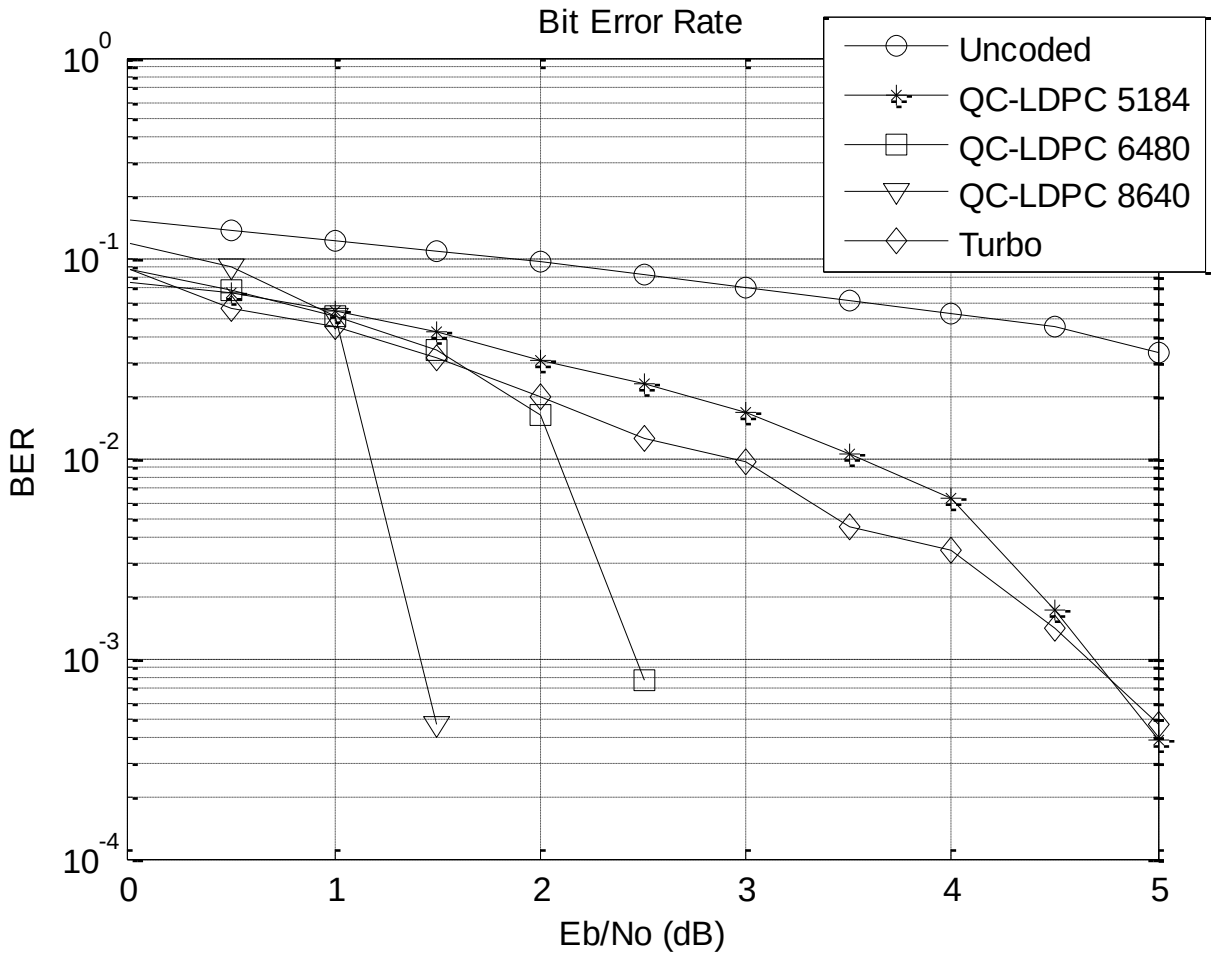

Figure 6-7. Comparison between turbo and QC-LDPC codes with G.hn standard

Table 6-5. Comparison between turbo and QC-LDPC codes with G.hn standard

	0	0.5	1	1.5	2	2.5	3	3.5	4	4.5
Uncoded	0.1543	0.1369	0.1221	0.1088	0.0957	0.0828	0.0711	0.0608	0.0532	0.0447
Turbo code	0.0867	0.0566	0.0453	0.0316	0.0200	0.0125	0.0095	0.0045	0.0034	0.0014
QC-LDPC 5184 (5/6)	0.0748	0.0660	0.0544	0.0428	0.0305	0.0237	0.0170	0.0106	0.0064	0.0017
QC-LDPC 6480 (2/3)	0.0872	0.0679	0.0509	0.0347	0.0162	0.0008	0	0	0	0
QC-LDPC 8640 (1/2)	0.1171	0.0892	0.0505	0.0005	0	0	0	0	0	0

6.5 Conclusions

In Chapter 6, we have designed QC-LDPC codes and compared with different block sizes and code rates. Because QC-LDPC codes are generated using circulant permutation of a base

matrix, the memory storage requirement can be reduced significantly. Moreover, encoding procedure is relatively simple and easy. The simulation with real channel noise is performed in Section 6.4. QC-LDPC codes with larger block sizes and low code rates generally outperform than codes with smaller block sizes and higher code rates in the simulation results. Furthermore, QC-LDPC codes with G.hn standard shows better BERs than turbo codes in most impulsive noise channels.

CHAPTER 7
FUTURE RESEARCH DIRECTION

Error Control Coding Comparison and Hybrid Decoder Design: We have designed and compared random LDPC and QC-LDPC codes with various block sizes and code rates. The comparison between turbo and LDPC codes are achieved on real PLC channels. As we can see the simulation results, QC-LDPC codes with large block size and low code rate outperform than the other codes generally. However, turbo code shows better results at low SNRs or specific channels. Moreover, we need more redundant bits for LDPC codes with low code rate. Even if its performance is better, it is not an efficient error code with low code rates. Therefore, it is important to find and design proper error control codes depending on channel condition.

Error control coding is still attentive research area and various schemes have been developed such as Reed-Solomon codes, convolutional codes, turbo codes, and LDPC codes with different code rates and size. In order to design and choose proper forward error correcting codes with performance improvement, we will try to design hybrid encoders and decoders with combing error correcting coding methods for the future research works. Therefore, LDPC codes and other error control codes are combined to improve bit error rates.

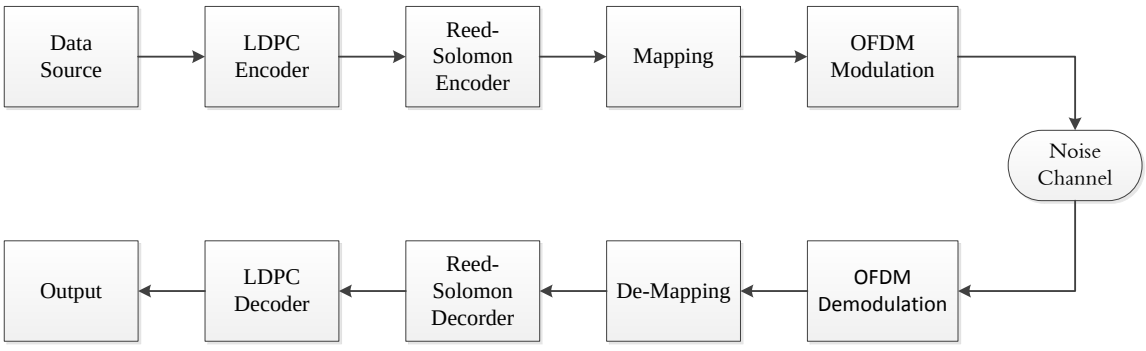

Figure 7-1. An example of hybrid error control codes with LDPC and Reed Solomon codes

Figure. 7.1 is the scenario of a hybrid error control coding scheme. It is designed with adapting LDPC code for outer code and as Reed-Solomon Code for inner code. We will design

various hybrid coding schemes and compare their performance. In addition to this, depending on channel condition, LDPC codes with flexible block size and code rates will be attempted.

Moreover, the hybrid decoding scheme which is combined sum-product with bit-flipping algorithm is possible to improve decoding performance. For the hybrid decoding scheme, first sum product decoding process is implemented, then bit flipping decoding process follows, and vice versa. As the modified decoding process is adopted without changing ending process, we can expect to enhance the performance than existing decoders. Generally more iteration process is required for the bit flipping algorithm than sum product algorithm. However, less iteration number is needed with the hybrid scheme than when each decoding scheme is applied separately. It is possible to reduce the processing time.

LIST OF REFERENCES

[1] B. Ji, A. Rao, M. Lee, H.A. Latchman, and S. Katar, "Multimedia in Home Networking," International Conference on Cybernetics and Information Technologies, July 2004.

[2] IEEE 802.11e/D6.0, Draft Supplement to Part 11: Wireless Medium Access Control (MAC) and physical layer (PHY) specifications: Medium Access Control (MAC) Enhancements for Quality of Service (QoS), Nov. 2003.

[3] S. Choi, "Emerging IEEE 802.11e WLAN for Quality-of-Service (QoS) Provisioning," Telecommuni-cations Review, vol. 12, no. 6, Dec. 2002.

[4] J. Haring and H. Vinck, "OFDM Transmission Corrupted by Impulse Noise," Proc. Int. Symp. Power Line Commun. Its Appl. (ISPLC), Limerick, Ireland, pp. 9-14, Apr. 2000.

[5] M. Ghosh, "Analysis of the Effect of Impulse Noise on Multicarrier and Single Carrier QAM Systems," IEEE Trans. Commun. vol. 44, No. 2, pp. 145-147, Feb. 1996.

[6] M. Zimmerman and K. Dostert, "Analysis and Modeling of Impulsive Noise in Broad-band Powerline Communications," IEEE Trans. Electro magn. Compat., vol. 44, pp. 249-257, Feb. 2002.

[7] V. Degardin, M. lienard, Z. Zeddam, F. Gauthier, and P. Degauque, "Classification and Characterization of Impulsive Noise on Indoor Power Line Used for Data Communications," IEEE Trans. Consum. Electron., vol. 48, No. 4, pp. 913-918, Nov. 2002.

[8] D. Middleton, "Statistical-physical models of electromagnetic interference," IEEE Trans. Electromagn. Compat., vol. 19, no. 3, pp. 106-127, Aug. 1977.

[9] N. Zogakis, P. S. Chow, J. T. Aslanis, and J. M. Cioffi, "Impulse Noise Mitigation Strategies for Multicarrier Modulation," Proc. IEEE Int. Conf. Commun, Geneva, Switzerland, vol. 2, pp. 784-788, 1993.

[10] M. Sliskovic, "Impulse Noise Detection Algorithms for Multicarrier Communication Systems-Performance Analysis," Proc. Int. Symp. Image Signal Processing Anal., Pula, Croatia, pp. 496-501, June 2001.

[11] S. V. Zhidkov, "Analysis and comparison of several simple impulsive noise mitigation schemes for OFDM receivers," IEEE Trans. Commun., vol. 56, no. 1, pp. 5–9, Jan. 2008.

[12] Mengi and A.J.H. Vinck, "Successive impulsive noise suppression in OFDM," Proc. IEEE Int. Symp. Power Line Commun. Its Appl. (ISPLC), pp. 33–37, March 2010.

[13] J. Cioffi, "A multicarrier primer," Tech. Rep. T1E1.4/91-157, Amati Comun. Corp. and Stanford University, 1991.

[14] R. G. Gallager, Low Density Parity Check Codes. Cambridge, MA, MIT Press, 1963.

[15] R. M. Tanner, “A recursive approach to low complexity codes,” IEEE Trans. Inform. Theory, vol. IT-27, pp. 533.547, Sept. 1981.

[16] D. MacKay and R. Neal, “Good codes based on very sparse matrices,” Cryptography and Coding, 5th IMA Conf., C. Boyd, Ed., Berlin, Springer-Verlag, Oct. 1995.

[17] D. MacKay, “Good error correcting codes based on very sparse matrices,” IEEE Trans. Inform. Theory, vol. 45, no. 3, pp.399-431, Mar. 1999.

[18] N. Alon and M. Luby, “A linear time erasure-resilient code with nearly optimal recovery,” IEEE Trans. Inf. Theory, vol. 42, no. 6, pp. 1732.1736, Nov. 1996.

[19] C. Berrrou, A. Glavieux, O. Thitimajshima, “Near Shannon Limit Error-Correcting Coding and Decoding: Turbo Codes,” Proceedings of International Conference on Communication, ICC'93, Geneva, Switzerland, p.1064-1070, 1993.

[20] G. Ungerboeck, “Channel coding with multilevel/phase signals,” IEEE Trans. Inf. Theory, vol. 28, no. 1, pp. 55-67, Jan. 1982.

[21] B. Rose, “Home Networks: A Standards Perspective,” IEEE Comm. Magn., vol. 39, issue 12, pp. 78-85, Dec. 2001.

[22] HomePNA Alliance, “No New Wires: Hitting a Winning Triple-Play Home Networking Solution,” http://www.homepna.org, Nov. 2006.

[23] HomePNA Alliance, “HomePNA and IPTV,” http://www.homepna.org, Apr. 2007.

[24] MoCA Alliance, “Enabling Service with MoCA,” www.mocalliance.org.

[25] “HomePlug AV White Paper,” http://www.homeplug.org, 2005.

[26] Homeplug Alliance, “Homeplug AV Specification,” May 2007.

[27] “802.11n: Next-Generation Wireless LAN Technology,” IEEE 802.11n White Paper, Apr. 2006.

[28] “Ultra-Wideband (UWB) Technology: Enabling high-speed wireless personal area etworks,” Ultra-Wideband (UWB) White Paper, http://www.intel.com/technology/ultrawideband, 2004.

[29] “Standard ECMA-368: High Rate Ultra Wideband PHY and MAC Standard 3rd edition,” http://ecma-international.org, Dec. 2008.

[30] “G.hn: Draft text for G.hn,” http://www.itu.int.

[31] “Telco TV Home Networking Technology and Market Outlook,” Independent Data and Analysis by S2 Data Corporation, Jan. 2007.

[32] ITU Telecommunication Sector, "Home networking transceivers - Enhanced physical, media access, and link layer specifications," hrrp://www.itu.int, Jan. 2007.

[33] B. Stascheit, "The Use of Ethernet-Over-Coax in HFC Networks," www.mocalliance.org, 2007.

[34] "Cable and Satellite Digital Entertainment Networks," Independent Data and Analysis by S2 Data Corporation, Apr. 2007.

[35] Monk, S. Palm, A. Garrett, R. Lee, and R. Leacock, "MoCA Protocols: What exactly is this MoCA thing?" www.mocalliance.org, Nov. 2007.

[36] S. Katar, M. Krishnam, R. Newman, and H. Latchman, "Harnessing the potential of powerline communications using the HomePlug AV standard," www.rfdesign.com, Aug. 2006.

[37] K. H. Afkhamie, S. Katar, L. Yonge, and R. Newman, "An Overview of the upcoming HomePlug AV standard," *2005 International Symposium on Power Line Comm. and Its Applications*, pp. 400-404, Apr. 2005.

[38] K. H. Afkhamie, S. Katar, L. Yonge, and R. Newman, "An Overview of the upcoming HomePlug AV standard," *2005 International Symposium on Power Line Comm. and Its Applications*, pp. 400-404, Apr. 2005.

[39] "Wi-Fi CERTIFIED 802.11n draft 2.0: Longer-Range, Faster-Throughput, Multimedia-Grade Wi-Fi Networks," *http://www.wi-fi.org*, 2007.

[40] V. Oksman, S. Galli, "G.hn: The New ITU-T Home Networking Standard," *IEEE Comm. Magn*, vol. 47, issue 10, pp. 138-145, Oct. 2009.

[41] K. J. Kerpez, "Minimum Mean Squared Error Impulse Noise Estimation and Cancellation," IEEE Trans. Signal Processing, Vol. 43, No. 7, pp. 1651-1662, July 1995.

[42] J. Armstrong and H. A. Suraweera, "Impulse Noise Mitigation for OFDM using Decision Directed Noise Estimation," Proc. IEEE Int. Symp. Spread Spectrum Tech. Appl., Sydney, Australia, pp.174-178, Aug. 2004.

[43] K. Seo and H. Latchman, "Improved Impulse Detection in Power Line Communication Systems," Proc. IEEE Int. Symp. Power Line Commun. Its Appl. (ISPLC), Jeju, Korea, pp 394-399, Apr., 2008.

[44] T. Wada, "A study on performance of LDPC codes on power line communications," Proceedings of IEEE International Conference on Communications, Vol. 1, pp. 109-113, June 2004.

[45] S. Galli, "On the Fair Comparison of FEC Schemes," Proceedings of IEEE International Conference on Communications, pp. 1-6, May 2010.

[46] P. Jagatheeswari and M. Rajaram, "Performance Comparison of LDPC Codes and Turbo Codes," European Journal of Scientific Research, Vol. 54, No.3, pp. 465-472, 2011.

[47] N. Ohkubo, N. Miki, Y. Kishiyama, K. Higuchi, and M. Sawahashi, "Performance Comparison Between Turbo Code and Rate-Compatible LDPC Code for Evolved Utra Downlink OFDM Radio Access," Proceedings of IEEE Military Communications Conference, pp. 1-7, Oct. 2006.

[48] C. Liu, Y. Shi, L. Wu, and Y. Pei, "Construction Method of LDPC Codes Used for Satellite Interactive System," Proceedings of Wireless Communications, Netwkring and Mobile Computing (WiCOM), pp. 1-3, Sep. 2011.

[49] T.Velmurugan, S.Balaji, A. S. Rennie, and D.Sumathi, "Efficiency of the LDPC Codes in the Reduction of PAPR in Comparison to Turbo Codes and Concatenated Turbo-Reed Solomon Codes in a MIMO-OFDM System," International Journal of Computer and Electrical Engineering (IJCEE), Vol. 2, No. 6, pp. 1005-1009, Dec. 2010.

[50] J. M. Cioffi, "A multicarrier primer," ANSI T1E1.4 Committee Contribution, pp. 91 - 157, 1991.

[51] W. Ryan and S. Lim, "Channel Codes: Classical and Modern," Cambridge University Press, 2009.

[52] Y. Kou , S. Lin, and M. Fossorier, "Low-density parity check codes based on finite geometries: a rediscovery and new results," IEEE Trans. Inform. Theory, vol. 47, pp.2711 -2736, 2001.

[53] R. M. Tanner , D. Sridhara , A. Sridharan , T. E. Fuja, and D. J. Costello, "LDPC block and convolutional codes based on circulant matrices," IEEE Trans. Inform. Theory, vol. 50, no. 12, pp.2966 -2984, 2004.

[54] M. P. C. Fossorier, "Quasi-cyclic low density parity check codes from circulant permutation matrices," IEEE Trans. Inform. Theory, vol. 50, pp.1788 -1794, 2004.

[55] N. Andreadou and F. Pavlidou, "QC-LDPC codes and their performance on Power Line Communications Channel," Proc. IEEE Int. Symp. Power Line Commun. Its Appl. (ISPLC), pp. 244–249, Apr. 2009.

[56] S. Myung, K. Yang, and J. Kim, "Quasi-cyclic LDPC codes for fast encoding," IEEE Trans. Inform. Theory, Vol. 51, issue 8, pp.2894-2901, Aug. 2005.

[57] H. Oh, Y. Park, S. Choi, J. Lee, and K. Whang, "Mitigation of Performance Degradation by Impulsive Noise in LDPC Coded OFDM System," IEEE ISPLC, pp.331–336, 2006.

[58] Robert H. Morelos - Zaragoza, "The Art of Error Correcting Coding, Second Edition," Wiley, 2006.

BIOGRAPHICAL SKETCH

Youngjoon Lee received his Bachelor of Science degree electrical engineering at Ajou University, South Korea in 2002 and his Master of Science in electrical and computer engineering at the University of Florida in 2005. He received his Ph.D. degree in electrical and computer engineering at the University of Florida in May 2013. He has worked on the area of communications and networks. Specifically, his main research topics are error control coding with LDPC codes, impulsive noise mitigation, home networks, and MAC protocol algorithm of WLAN and PLC.